Supporting Online Material

This material includes:

- Materials and Methods
- Movies (movie S1-S8)
- Movie Legends
- Supplemental figures (fig. S1-S21)
- Supplemental figure legends
- References for Supporting Online Material

Materials and Methods

Bioinformatics. BLAST searches of *Drosophila* genome release v5.16 (*1*) using human Sesn1-3 protein sequences resulted in identification of open reading frame CG11299 as a unique Sesn homologue. The phylogenetic tree in fig. S1A was constructed using Neighbor-Joining algorithm, and the branch lengths indicate evolutionary distance. Multiple protein sequence alignment in fig. S1B was done with the CLUSTALW algorithm and shaded using GeneDoc v2.5. Drawing of schematic genomic organization and identification of transcription factor binding sites were performed using GenePalette v2.0.

Generation of *dSesn* mutants. Flybase database search indicated that the *P(XP)d04539* fly line in the Harvard/Exelixis stock collection has an XP element [a modified EP element with bidirectional UAS insertions (*2*)] insertion in the 5'-untranslated region of the *dSesn* gene. PCR analysis verified the location and direction of the XP element insertion to be accurate. After confirming stimulation of dSesn expression by GAL4 after crossing with GAL4 lines (fig. S2), *P(XP)d04539* was designated as a GAL4-activatable *dSesn* allele, $dSesn^{XP4}$.

The UAS in the $dSesn^{XP4}$ allele was deleted by crossing $dSesn^{XP4}$ males (P) with *y w hs-Flp;* noc^{Sco}*/CyO* virgins, and the F_1 progenies were heat-shocked twice at 37°C for 1 hr during the first and second instar larval stages. F_1 males were crossed with *w; In(2LR)* wg^{Gla} Bc^{1}*/CyO* females, and red-eyed F_2 males were subjected to single pair backcrosses with *w; In(2LR)* wg^{Gla} Bc^{1}*/CyO* females. Each independent line produced from single pair matings (s.p.m.) was screened for deletions of the UAS by genomic PCR

using primers flanking the FRT-UAS-FRT sequences of the XP element, 5'-CACCTGCAAAAGGTCAGACA-3' (forward) and 5'-AATTCGGCTGCTGCTCTAAA -3' (reverse). The modified *dSesn*^{XP4} line with a UAS deletion was designated as *dSesn*$^{XP4\Delta UAS}$.

The LD39604 cDNA clone, which contains full-length *dSesn* cDNA, was obtained from *Drosophila* Genome Research Center (Indiana). Cys86 of dSesn which is critical for its antioxidant function (*3*) was converted to a Ser using QuikChange II Site-Directed Mutagenesis Kit (Stratagene) to produce *dSesn*^{CS}. *dSesn*^{WT} and *dSesn*^{CS}, as well as *mSesn1* and *mSesn2* coding sequences were subcloned into pUAST (*4*) after fusion to an N-terminal Myc epitope (MEQKLISEEDL) and a Kozak sequence (5'-GCCACC-3'). The cloned constructs were microinjected with helper plasmids into *w*^{1118} embryos to produce the corresponding transgenic flies (Rainbow transgenic flies, Inc.). Two transgenic insertions per each construct, in the second and third chromosomes were isolated and balanced.

dSesn-null alleles were generated using imprecise excision by crossing the *dSesn*^{XP4} line with a *w*$^{+}$*Δ2-3* transposase line (4 to 6 bottles). Resulting *dSesn*^{XP4}/*w*$^{+}$*Δ2-3* F_1 males were crossed with *w*; *In(2LR) wg*^{Gla} *Bc*^{1}*/CyO* virgins (400 s.p.m. crosses), and white-eyed F_2 males were selected and backcrossed with *w; In(2LR) wg*^{Gla} *Bc*^{1}*/CyO* virgins (1,600 s.p.m. crosses). Each male from the final s.p.m. was collected 7 days after crosses, and screened by PCR for *dSesn* deletions using primers that flank the *dSesn*^{XP4} insertion site with 2-4 kb intervals in the *dSesn* locus. The LA-PCR system (Sigma) was used to increase the sensitivity of the screen, according to the manufacturer's

recommendations. The final screen identified a series of genomic *dSesn* deletion alleles, including *dSesn*^{8A11} and *dSesn*^{3F6} that were used in this study (fig. S4).

Fly stocks. Balancer lines, Transposase lines, FLP-FRT lines, GAL4 lines, *UAS-InR*^{CA}, *UAS-InR*, *UAS-InR*^{DN}, *UAS-Rheb*, *UAS-PI3K*^{CA}, *UAS-PI3K*^{DN}, *UAS-AKT*, *UAS-S6k*^{CA}, *UAS-S6k*, *UAS-S6k*^{DN}, *UAS-Tor*^{DN}, *UAS-Thor*^{CA}, *UAS-p53*^{DN}, *UAS-JNK*^{DN}, *UAS-catalase*, *UAS-FoxO*, *UAS-p53*, *UAS-Mkk7*^{CA}, *UAS-Dcr2*, *UAS-dATG1*^{RNAi}, *p53*$^{5A-1-4}$, *Thor*^{1} were received from the Bloomington Stock center. *Pten*^{3} and *UAS-Pten* (*5*), *UAS-Mst1* and *UAS-Mst1*^{DN} (*6*), *Tsc1*^{Q87X} *(7, 8)*, *FoxO*^{21} and *FoxO*^{25} (*8, 9*), *hand-GAL4* (*10*), *UAS-dSesn*^{RNAi} and *UAS-dAMPK*^{RNAi} (*11*) were previously described. *Tsc2*$^{E1.16}$ is a loss-of-function *Tsc2* allele obtained from I. Hariharan (UC Berkeley). *UAS-TSA* (peroxiredoxin) was previously generated in E. Bier's laboratory. *gmr-GAL4 FoxO*^{21} and *UAS-Rheb*$^{EP50.084\text{-}loxP}$ *FoxO*^{25} double mutant strains were obtained from S. Oldham (Burnham institute).

Genotypes. Fig. 1: (A and D) *ap-GAL4/+*, (B and E) *ap-GAL4/UAS-InR*^{CA}, (C) *ap-GAL4 dSesn*^{8A11}*/UAS-InR*^{CA} *dSesn*^{8A11}, (G) *ap-GAL4/UAS-Rheb*, (J) *ap-GAL4*/*UAS-S6k*^{CA}, (K) *Thor*^{1}, (H) *y w hsp70-FLP*; *FRT40A Ubi-GFP*^{33} *Ubi-GFP*^{38}*/FRT40A Pten*^{3}, (I) *y w hsp70-FLP*; *FRT82B Ubi-GFP*^{83}*/FRT82B Tsc1*^{Q87X}. **Fig. 2:** (A) *ap-GAL4/+*, *ap-GAL4/UAS-InR*^{CA} and *ap-GAL4/UAS-Rheb*, (C and F) *y w hsp70-FLP*; *FRT82B Ubi-GFP*^{83}*/FRT82B Tsc1*^{Q87X}, (B) *gmr-GAL4*/+, *gmr-GAL4 UAS-InR*^{CA}/+, *gmr-GAL4/UAS-Rheb*, *UAS-PI3K*^{DN}/Y; *gmr-GAL4 UAS-InR*^{CA}/+, *gmr-GAL4 UAS-InR*^{CA}*/UAS-Tor*^{DN}, *gmr-GAL4 UAS-InR*^{CA}*/UAS-S6k*^{DN} and *gmr-GAL4 UAS-InR*^{CA}/+; *UAS-Thor*^{CA}/+, (D) *gmr-GAL4*/+, *gmr-GAL4/UAS-InR*^{CA}, *gmr-GAL4 UAS-InR*^{CA}*/UAS-TSA*, *gmr-GAL4 UAS-*

InR^{CA}/*UAS-catalase*, (E) *ap-GAL4/UAS-InR*^{CA} and *ap-GAL4 UAS-catalase/UAS-InR*^{CA}. **Fig. 3:** (A) *gmr-GAL4*/+, (B) *gmr-GAL4 dSesn*^{XP4}/+, (C) *gmr-GAL4*/*UAS-InR*^{CA}, (D) *gmr-GAL4 dSesn*^{XP4}/*UAS-InR*^{CA}, (E) *gmr-GAL4*/*UAS-Rheb*, (F) *gmr-GAL4 dSesn*^{XP4}/*UAS-Rheb*, (I) *ap-GAL4*/*UAS-InR*, (J) *ap-GAL4*/*UAS-AKT*, (K) *ap-GAL4 dSesn*^{XP4}/*UAS-InR*, (L) *ap-GAL4 dSesn*^{XP4}/*UAS-AKT*, (M) *ap-GAL4 dSesn*^{8A11}/*UAS-InR dSesn*^{8A11}, (N) *ap-GAL4 dSesn*^{8A11}/*UAS-AKT dSesn*^{8A11}. Genotypes in G and H were same as corresponding genotypes in A to F. **Fig. 4:** (A, C to E) *w*^{1118} and *dSesn*^{8A11}, (B) *dSesn*^{8A11}/+; *hs-GAL4*/+, *dSesn*^{8A11}; *hs-GAL4*/+, *dSesn*^{8A11}; *hs-GAL4 UAS-Myc-dSesn*^{WT}/+ and *dSesn*^{8A11}; *hs-GAL4*/*UAS-Myc-dSesn*^{CS}. **Fig. 5:** *w*^{1118}, *dSesn*^{8A11} and *dSesn*^{8A11}/*dSesn*^{8A11} *UAS-catalase*; *hs-GAL4*/+ **Fig. 6:** (A) *dSesn*^{8A11}/+, (B) *dSesn*^{8A11}/*dSesn*^{3F6}, (C, E, F and G) *dSesn*^{8A11}, (D) *dSesn*^{8A11}; *hs-GAL4*/*UAS-Myc-dSesn*^{CS}. **Fig. 7:** (A) *hand-GAL4/+*; *hand-GAL4 UAS-GFP/+*, (B) *hand-GAL4/+*; *hand-GAL4 UAS-GFP/UAS-dATG1*^{RNAi}, (D) *UAS-Dcr2/+*; *Mef2-GAL4/+*; *UAS-dATG1*^{RNAi}/+, (E) *ap-GAL4/+* and *ap-GAL4/+*; *UAS-dATG1*^{RNAi}/+. Genotypes in C were same as corresponding genotypes in A and B. For detailed genotypes of flies used in Supplemental figures, see Supplemental figure legends.

Clonal analyses. *y w hsp70-FLP*; *FRT40A Ubi-GFP*^{33} *Ubi-GFP*^{38}/*CyO* females were crossed to *FRT40A Pten*^{3}/*CyO* males to produce larvae with *Pten*-null clones. *y w hsp70-FLP*; *FRT82B Ubi-GFP*^{83}/*TM3 Sb*^{1} females were crossed to *FRT82B Tsc1*^{Q87X}/*TM6B* males to produce larvae with *Tsc1*-null clones. After overnight egg collection, the first instar larvae were heat shocked at 37°C for 1 hr. Third instar larval wing discs with variegated GFP pattern were analyzed by dSesn immunostaining or DHE staining.

Generation of anti-dSesn antibodies. Full-length *dSesn* cDNA was cloned into pGEX, and transformed into *E. coli BL21*. GST-dSesn fusion protein purified on a GST-agarose column (Bio-Rad) was injected repeatedly into rabbits with Freund's adjuvant (Sigma) at 3-4 week intervals. After 9 injections, sera were collected and subjected to affinity purification using PVDF-immobilized GST-dSesn. Purified antibodies were concentrated using a Centricon column (Millipore) and further cleared by pre-absorption with fixed *dSesn*-null ($dSesn^{8A11}$) homozygous embryos.

Antibodies. Anti-Wingless (4D4, DSHB), anti-Elav (7E8A10, DSHB), anti-actin (Amersham), anti-alpha tubulin (B-5-1-2, Sigma), anti-Flag (M2, Sigma), anti-Myc (9E10, Santa Cruz), anti-S6K (Santa Cruz), anti-p53 (Santa Cruz), anti-HA (3F10, Roche), anti-digoxigenin (Roche), anti-phospho S6K (Thr389) (Cell Signaling), anti-phospho *Drosophila* S6K (Thr398) (Cell Signaling), anti-phospho 4E-BP (Thr37/46) (Cell Signaling), anti-phospho JNK (Thr183/Tyr185) (Cell Signaling), anti-Ubiquitin (Upstate), anti-phospho *Drosophila* AKT (Ser509) (Cell Signaling), anti-phospho AKT (Ser473) (Cell Signaling), and anti-*Drosophila* FoxO (a gift from O. Puig and M. Tatar) were used for immunostaining and immunoblot analyses.

Immunostaining. Third instar wandering-stage larvae of the indicated genotypes identified by genetic markers (Bc^1 for second chromosome and Tb^1 for third chromosome) were collected, washed and dissected in phosphate-buffered saline (PBS). Imaginal disc complexes were fixed in Brower Fix (0.15 M PIPES pH 6.9, 3 mM $MgSO_4$, 1.5 mM EGTA, 1.5% NP40) mixed with 1/3 volume of 8% methanol-free formaldehyde for 3 hrs at 4°C. After washing in PBS plus 0.1% Tween20 (PBT), the fixed tissues were

incubated in a blocking solution composed of PBT plus 1X Western blocking reagent (Roche) for 1 hr at room temp. The tissues were then incubated overnight at 4°C with primary antibodies appropriately diluted in the blocking solution. The tissues were then washed with PBT, and incubated for 3 hrs at room temperature with fluorophore-conjugated secondary antibodies (Molecular Probes, Invitrogen) that were diluted in blocking solution. After washing with PBT and PBS, the tissues were mounted in ProLong Gold anti-fade reagent (Invitrogen). If needed, TRITC-labeled phalloidin (Sigma) was added at the primary antibody incubation step and DAPI (Sigma) or TO-PRO-3 (Invitrogen) were added at the final washing step. Samples were examined under an epifluorescence-equipped (Zeiss) or laser confocal (Leica/Zeiss) microscope.

Preparation of DIG-labeled RNA probe for dSesn. Pfu PCR (Stratagene) was performed to amplify the 219 bp 5'-UTR fragment of *dSesn* exon 3, using 5'-CAACATCTGAGGAGCACAAG-3' as a forward primer, 5'–TAATACGACTCA CTATAGGGAGCGGAATATCCGAGGTC-3' as a reverse primer, and w^{1118} genomic DNA as a template. Since the reverse primer contains a T7 linker, the PCR product can serve as a template for RNA synthesis. DIG-labeled RNA probe was generated using DIG RNA labeling kit (T7, Roche) according to manufacturer's instructions. The RNA probe was purified using Megaclear RNA purification kit (Ambion) and its quality and quantity were determined by agarose gel electrophoresis and spectroscopy, respectively.

Simultaneous detection of mRNA and protein. A protocol for simultaneous detection of mRNA and protein was modified from a previous one (*12*) as follows: Imaginal disc complexes were isolated and fixed as for immunostaining. Fixed tissues

were washed twice with PBT, 4 times with methanol (MeOH), 5 times with ethanol (EtOH), and stored at -20°C overnight. On the following day, the tissues were washed 3 times with EtOH and incubated in 50% Xylene in EtOH for 30 min. Then, the tissues were washed 5 times with EtOH, 2 times with MeOH, and fixed in 5% formaldehyde in PBT for 30 min. The samples were washed 5 times with PBT and incubated with 10 μg/mL proteinase K in PBT for 5 min. The samples were then washed 4 times with PBT and fixed again in 5% formaldehyde in PBT for 30 min, followed by 5 washes with PBT. The tissues were then washed once with 50% hybridization solution (Hyb) in PBT and 4 times with Hyb (50% deionized formamide, 5X SSC, 100 μg/mL sheared salmon sperm DNA, and 50 μg/mL heparin). The tissues in Hyb were then transferred to a 55°C incubator and incubated for 2 hrs with gentle shaking. 10 ng of DIG-labeled *dSesn* probe, prepared as described above, diluted in 200 μl of Hyb, were added to the tissues, and incubated for 2 days at 55°C with gentle shaking. After incubation, the tissues were washed once with Hyb and 5 times with 50% Hyb in PBT for 20 min each at 55°C. The tissues were then washed 5 times with PBT and subjected to anti-DIG and anti-Wg immunostaining as described above.

ROS detection and measurements. In vivo detection of ROS was performed according to a previously described protocol (*13*) using dihydroethidium (DHE) dye (Molecular Probes, Invitrogen), and the images were taken under an epifluorescence-equipped microscope (Zeiss) or a laser confocal microscope (Zeiss) without fixation. For *cis*-aconitase assay, thirty adult males were homogenized in 120 μl of extraction buffer (0.6 mM $MnCl_2$, 2 mM citric acid, 50 mM Tris-HCl, pH 8.0) and centrifuged at 16,000 x

g. 2 μL samples of clarified extracts were mixed with 800 μL of 100 mM potassium phosphate, pH 6.5, 1 mM NADPH, 2 mM *cis*-aconitic acid, 1.2 mM 3-(4,5-dimethylthiazol-2-yl)-2,5-diphenyl tetrazolium bromide (MTT), 0.3 mM phenazine methosulfate (PMS), 25 mM $MgCl_2$, 5 units/ml isocitrate dehydrogenase, and absorbance at 570 nm was recorded every 30 seconds at 25°C. In this system, isocitrate produced by *cis*-aconitase was further converted by isocitrate dehydrogenase, in the presence of NADP, Fe^{2+}, MTT and PMS, to a chromogenic product (*14*).

Mammalian cell culture. For transient expression in mammalian cells, *dSesn* full-length cDNA was cloned into pLV-CMV after fusion to an N-terminal Myc epitope and a Kozak sequence. Cell lines, all other constructs and procedures were described (*15*).

Immunoblotting. For head proteins, 20 to 50 heads from each fly strain were collected and homogenized in cell lysis buffer (20 mM Tris-Cl pH 7.5, 150 mM NaCl, 1 mM EDTA, 1 mM EGTA, 2.5 mM NaPPi, 1 mM β-glycerophosphate, 1 mM Na_3VO_4, 1% Triton-X-100). For whole adult proteins, 10-days-old male flies were homogenized in cell lysis buffer. For larval fat body proteins, fat bodies were dissected from 10 third instar larvae and homogenized in cell lysis buffer. Lysates were clarified by centrifugation, boiled in 1X SDS sample buffer, resolved by SDS-PAGE, transferred onto PVDF membranes and probed with the relevant antibodies as described (*15*). Chemiluminescence was detected using X-ray film (Phenix) or Versadoc system (Bio-rad), and luminosity from the inverted film image whose background was set as a black reference was measured.

Southern/Northern blotting. DNA extracted using the DNeasy system (Qiagen) was digested with indicated restriction enzymes and separated on a TAE-agarose gel. After depurination, denaturation and neutralization, the gel was blotted onto Hybond-N^+ membranes (Amersham). Total RNA extracted using the Trizol system (Invitrogen) was separated on a MOPS-formaldehyde-agarose gel and blotted onto Hybond-N^+ membranes. Full-length *dSesn* cDNA and PCR fragments of *rp49* amplified from genomic DNA with 5'-AATGGTGCTGCTATCCCAAT-3' (forward primer) and 5'-GGTTTCCGGCAAGGT ATGT-3' (reverse primer) were used as probe templates. Blot hybridization was as described (*15*).

Quantitative RT-PCR. RNA extracted as above was reverse-transcribed using MMLV-RT (Promega) with random hexamers (Invitrogen). Relative transcript amounts were measured by an iCycler iQ Real-Time PCR system (Biorad). RT-PCR primers: *rp49*, 5'-ACGTTGTGCACCAGGAACTT-3' (forward) and 5'-CCAGTCGGATCGATAT GCTAA-3' (reverse); *dSesn*, 5'-CTCGACTCGATCCCTCCG-3' (forward) and 5'-CAGGTCATCGAGCTCGTCC-3' (reverse); *dAMPK*, 5'-CATCCGCACAT CATCAAGTT-3' (forward) and 5'-TTCTCTGGCTTCAGGTCTCG-3' (reverse); *dSREBP*, 5'-CGCAGTTTGTCGCCTGATG-3' (forward) and 5'-CAGACTCCTGTCCAAGAGCTGTT-3'; *dPGC-1*, 5'-GGATTCACGAATGCTAAA TGTGTTCC-3' (forward) and 5'-GATGGGTAGGATGCCGCTCAG-3' (reverse); *lip3*, 5'-GATGGCTACCCGATGGAGCGC-3' (forward) and 5'-CGGTCGGTTGGAA GATTCACCC-3' (reverse); *CG5966*, 5'-GGCCAACCACACCAGTCGGG-3' (forward) and 5'-GTGTTCCAGGGTCCATTGATCGG-3' (reverse); *CG11055*, 5'-GT

TCGCATGCGGAAATCACACTGC-3' (forward) and 5'-GAGAACTCCGCGTAT CGAGTCG-3' (reverse); *dACC*, *dACS*, *dFAC* and *dFAS* primers were designed as described (*16*).

Nile Red staining. Nile Red staining was done as described (*17*).

Triglyceride measurement. For quantification of triglycerides, crude lysates of five 10-day-old adult male flies in PBS were prepared by sonication. Triglyceride amounts were measured using Triglyceride-SL assay kit (Genzyme Diagnotics) according to manufacturer's instructions, and normalized to protein amounts measured by the Bio-Rad protein assay kit (Biorad).

Adult wing analysis. Adult wings were dissected and mounted in Gary's magic mountant (GMM, 50% canadian balsam in methyl salicylate). Anterior views of adult wings were taken under Leica MZ8 dissection microscope and processed to remove non-essential body parts including legs and abdomens.

Drug feeding. Metformin (Sigma), 5-aminoimidazole-4-carboxamide-1-β-D-ribofuranoside (AICAR, TRC chemicals) and rapamycin (LLC chemicals) were dissolved in 300 μL PBS at a concentration of 100 mM (AICAR and metformin) or 1μM (rapamycin), and absorbed into normal fly medium as previously described (*18*). Vitamin E dissolved in ethyl acetate was mixed with normal medium at concentration of 20 μg/mL (*19*) and dried under room temperature overnight until the solvent smell was gone. For Fig. 2F, vitamin E was mixed with normal medium at a concentration of 200 μg/mL.

Electron microscopy. Scanning electron micrographs were taken using Phillips

XL30 ESEM in an environmental mode at Calit2-Nano3 facility. Five non-overlapping areas in the central region of a single SEM image, each with 7 ommatidia, were selected and used for ommatidial size measurement. For transmission electron micrographs, pieces of *Drosophila* thoracic tissues were fixed in 2% paraformaldehyde plus 2.5% glutaraldehyde (Ted Pella, Redding, CA) in 0.1 M sodium cacodylate (pH 7.4) on ice for 1 hr. The samples were washed three times with buffer consisting of 0.1 M sodium cacodylate plus 3 mM calcium chloride (pH 7.4) on ice and then post-fixed with 1% osmium tetroxide, 0.8% potassium ferrocyanide, 3 mM calcium chloride in 0.1 M sodium cacodylate (pH 7.4) for 1 hr, washed three times with ice-cold distilled water, en bloc stained with 2% uranyl acetate at 4°C for 1 hr, dehydrated through graded ethanol solutions, and embedded in Durcupan ACM resin (Fluka, St. Louis, MO). Ultrathin (80 nm) sections were post-stained with uranyl acetate and lead salts prior to imaging using a JEOL 1200FX transmission EM operated at 80 kV. The negatives were digitized at 1800 dpi using a Nikon CoolScan system, giving an image size of 4033 x 6010 pixels and a pixel resolution of 1.77 nm.

TUNEL staining. TUNEL staining was performed using an In Situ Cell Death Detection Kit (TMR Red, Roche) according to manufacturer's instructions, using a whole mount method.

Fly heartbeat analysis. For heart parameter measurements, semi-intact fly heart preparation was prepared according to a previously described protocol (*20*). High speed 1 minute movies were taken at a rate of >100 frames per second using a Hamamatsu CCD camera on a Leica DM LFSA microscope with a 10x dipping immersion lens. The images

were processed using Simple PCI imaging software (Hamamatsu Inc.). M-modes and quantitative data were generated using a MatLab-based image analysis program (*20, 21*). Briefly, to generate M-mode figure, a single pixel-wide column that encompasses both edges of the heart tube was selected, and corresponding columns were cut from all movie frames and aligned horizontally according to time. Thus, the M mode provides an edge trace that documents the movement of the heart tube walls in the *y*-axis over time in the *x*-axis. An arrhythmia index was calculated as the standard deviation of all recorded heart periods normalized to the median heart period for each individual fly, since large standard deviations in heart periods for a single fly are a reflection of nonrhythmic contraction/relaxation cycles. Heart periods are defined as the time between the ends of two consecutive diastolic intervals.

Movie legends

Movie S1. Cardiac dynamics of 2-week-old adult female w^{1118} *Drosophila*.

Movie S2. Cardiac dynamics of 2-week-old adult female $dSesn^{8A11}$ *Drosophila*.

Movie S3. Cardiac dynamics of 2-week-old adult female $dSesn^{8A11}$ *Drosophila* fed with 100 mM AICAR.

Movie S4. Cardiac dynamics of 2-week-old adult female $dSesn^{8A11}$ *Drosophila* fed with 1 μM rapamycin.

Movie S5. Cardiac dynamics of 2-week-old adult female *hand-GAL4*/+; *hand-GAL4 UAS-GFP*/+ *Drosophila*.

Movie S6. Cardiac dynamics of 2-week-old adult female *hand-GAL4*/+; *hand-GAL4 UAS-GFP/UAS-*$dSesn^{RNAi}$ *Drosophila*.

Movie S7. Cardiac dynamics of 2-week-old adult female *hand-GAL4/UAS-*$dAMPK^{RNAi}$; *hand-GAL4 UAS-GFP*/+ *Drosophila*.

Movie S8. Cardiac dynamics of 2-week-old adult female *hand-GAL4*/+; *hand-GAL4 UAS-GFP/UAS-*$dATG1^{RNAi}$ *Drosophila*.

Supplemental figure legends

fig. S1. Identification of *Drosophila* Sestrin (dSesn). (**A**) Phylogenetic tree analysis of the relationship between dSesn, *C. elegans* Sesn (cSesn) and human Sesns (hSesn1-3). (**B**) Sequence alignment of dSesn, cSesn and hSesn1-3. (**C**) Expression of dSesn. Flies of the indicated developmental stages were analyzed by Northern blotting using *dSesn* and *rp49* probes. 28S rRNA was visualized by ethidium bromide staining (left panel). In addition, lysates of 1.5- and 6-week-old adults were analyzed by immunoblotting using dSesn and tubulin antibodies (right panel).

fig. S2. Overexpression of dSesn from the $dSesn^{XP4}$ allele. (**A**) Schematic genomic organization of the *dSesn* locus and the $dSesn^{XP4}$ UAS insertion. $dSesn^{XP4}$, originally named *P(XP)d04539*, has an XP element (*2*) insertion in the 5'-untranslated region of *dSesn*. (**B** to **D**) *hs-GAL4* stimulates expression of the $dSesn^{XP4}$ allele. Adult *hs-GAL4*/+ (*hs-GAL4*) and $dSesn^{XP4}$/+; *hs-GAL4*/+ (*hs*>$dSesn^{XP4}$) males were heat-shocked at 37°C for 1 hr to express GAL4 and left to recover at 25°C for 3 hrs, after which total RNA was extracted and subjected to Northern blotting with *dSesn* and *rp49* probes (B), and quantitative RT-PCR analysis for *dSesn* transcripts, normalized to *rp49* transcripts (C). Protein lysates were analyzed by immunoblotting with the indicated antibodies (D). (**E**) *gmr-GAL4*-stimulated $dSesn^{XP4}$ expression. Third instar larval eye imaginal discs of *gmr-GAL4*/+ (*gmr-GAL4*) and *gmr-GAL4*/$dSesn^{XP4}$ (*gmr*>$dSesn^{XP4}$) flies were immunostained with anti-dSesn antibody (green). (**F**) *ap-GAL4*-stimulated $dSesn^{XP4}$ expression. Third

instar larval wing imaginal discs of *ap-GAL4*/+ (*ap-GAL4*) and *ap-GAL4*/*dSesn*^{XP4} (*ap>dSesn*^{XP4}) flies were immunostained with anti-dSesn antibody (green).

fig. S3. Sestrin-expressing transgenic flies. (**A**) Adult *hs-GAL4*/+ (*hs-GAL4*), *UAS-Myc-dSesn*^{WT}/+; *hs-GAL4*/+ (*hs>Myc-dSesn*^{WT}) and *UAS-Myc-dSesn*^{CS}/+; *hs-GAL4*/+ (*hs>Myc-dSesn*^{CS}) male flies were heat-shocked at 37°C for 1 hr to express GAL4, allowed to recover at 25°C for 3 hrs, homogenized and analyzed by immunoblotting with the indicated antibodies. (**B** to **F**) Third instar larval wing imaginal discs of *ap-GAL4*/+ (*ap-GAL4*) and *ap-GAL4*/*UAS-Myc-dSesn*^{WT} (*ap>Myc-dSesn*^{WT}), *ap-GAL4*/*UAS-Myc-dSesn*^{CS} (*ap>Myc-dSesn*^{CS}), *ap-GAL4*/*UAS-Myc-mSesn1* (*ap>Myc-mSesn1*), *ap-GAL4*/*UAS-Myc-mSesn2* (*ap>Myc-mSesn2*) flies were immunostained with anti-Myc antibody (green) to detect expression of Myc-tagged Sesn proteins.

fig. S4. Generation of *dSesn*-null mutants. (**A**) Schematic genomic organization of the *dSesn* locus and the *dSesn*-null mutant. Brackets indicate the genomic deficiency in the *dSesn*-null alleles, which span bp 19,601,349 to 19,621,707 (*dSesn*^{8A11}) and 19,600,761 to 19,604,679 (*dSesn*^{3F6}) of chromosome 2R (*Drosophila* genome release v5.16). Gray boxes: untranslated exons; black boxes: protein-coding exons; white arrow: open reading frame *CG18218*. (**B**) Absence of *dSesn* coding sequence (CDS) in *dSesn*^{8A11} flies. Genomic DNAs from wild type (+/+), *dSesn*^{8A11}/+ (+/-) and *dSesn*^{8A11}/*dSesn*^{8A11} (-/-) adults were digested with the indicated restriction enzymes and analyzed by Southern blotting (SB) with *dSesn* CDS and *rp49* probes. (**C**) Absence of dSesn protein in *dSesn*-

null flies. Protein samples from wild type (*dSesn*$^{+/+}$), *dSesn*^{8A11}/*dSesn*^{8A11} (*dSesn*^{8A11}), and *dSesn*^{8A11}/*dSesn*^{3F6} (*dSesn*$^{8A11/3F6}$) adults were gel separated and immunoblotted with anti-dSesn and anti-tubulin antibodies.

fig. S5. InR^{CA} increases dSesn expression by activating TOR. Third instar larval eye imaginal disc expressing the indicated genetic elements were immunostained for dSesn (green) and Elav (red). Genotypes: *gmr-GAL4*/+ (*gmr*-Con), *gmr-GAL4 UAS-InR*^{CA}/+ (*gmr>InR*^{CA}), *UAS-PI3K*^{DN}/Y; *gmr-GAL4 UAS-InR*^{CA}/+ (*gmr>InR*^{CA}+*PI3K*^{DN}), *gmr-GAL4 UAS-InR*^{CA}/*UAS-Tor*^{DN} (*gmr>InR*^{CA}+*Tor*^{DN}), *gmr-GAL4 UAS-InR*^{CA}/*UAS-S6k*^{DN} (*gmr>InR*^{CA}+*S6k*^{DN}), *gmr-GAL4 UAS-InR*^{CA}/+; *UAS-Thor*^{CA}/+ (*gmr>InR*^{CA}+*Thor*^{CA}).

fig. S6. FoxO stimulates dSesn expression. (**A**) Genomic organization and location of FoxO response elements (FRE, GTAAACAA (*22*)) in the *dSesn* locus. Forward FREs are indicated in red and reverse FREs in blue. (**B** to **F**) Third instar larval eye imaginal discs of *gmr-GAL4*/+ (B), *gmr-GAL4*/*UAS-FoxO* (C), *gmr-GAL4*/*UAS-p53* (D), *gmr-GAL4 p53*$^{5A-1-4}$/*UAS-InR*^{CA} *p53*$^{5A-1-4}$ (E), *gmr-GAL4 FoxO*^{25}/*UAS-InR*^{CA} *FoxO*^{21} (F) flies were immunostained for dSesn (green) or Elav (red) as indicated. (**G** and **H**) Third instar larval eye imaginal discs of *gmr-GAL4*/*UAS-Rheb*$^{EP50.084-loxP}$ *FoxO*^{25} (G) and *gmr-GAL4 FoxO*^{21}/*UAS-Rheb*$^{EP50.084-loxP}$ *FoxO*^{25} (H) flies were immunostained for dSesn (red) or Elav (green) as indicated. (**I** and **J**) Third instar larval wing imaginal discs of *ap-GAL4*/*UAS-InR*^{CA} (I) and *ap-GAL4 FoxO*^{25}/*UAS-InR*^{CA} *FoxO*^{21} (J) were immunostained for dSesn (green) and Wg (red). (**K** to **M**) Third instar larval wing imaginal discs of *ap-*

GAL4/+ (K), *ap-GAL4*/*UAS-InR*^{CA} (L) and *ap-GAL4*/*UAS-Rheb* (M) were immunostained for FoxO (green). Nuclei were visualized by TO-PRO-3 staining (red). Dorsoventral boundary, inferred from Wg staining, is indicated by the dotted line. Dorsal side is to the left as indicated (D-V).

fig. S7. JNK mediates accumulation of dSesn in response to expression of InR^{CA} (**A** to **C**) InR^{CA} activates JNK through the accumulation of ROS. Third instar larval wing discs of *ap-GAL4*/+ (A), *ap-GAL4*/*UAS-InR*^{CA} (B) and *ap-GAL4 UAS-catalase*/*UAS-InR*^{CA} (C) were stained with anti-phospho JNK (green) and anti-Wg (red) antibodies. (**D** to **H**) Accumulation of dSesn is JNK-dependent. Third instar larval eye discs of *gmr-GAL4*/+ (D), *gmr-GAL4*/+; *UAS-Mkk7*^{CA}/+ (E), *gmr-GAL4*/+; *UAS-Mst1*/+ (F), *UAS-JNK*^{DN}/Y; *gmr-GAL4 UAS-InR*^{CA}/+ (G), *gmr-GAL4 UAS-InR*^{CA}/+; *UAS-Mst1*^{DN}/+ (H) were stained for dSesn (green) or Elav (red) as indicated.

fig. S8. dSesn suppresses tissue growth by reducing cell size. (**A** to **F**) Expression of dSesn causes wings to bend upwards. The indicated genetic elements were specifically expressed in the dorsal wing using an *ap-GAL4* driver. (**G** and **H**) Expression of dSesn reduces cell size. Dorsal views of wings with or without dSesn expression. Pink-shaded wing regions bounded by L3, L4, C1 and extrapolated C2 veins were used to calculate cell size and number. (**I** to **K**) Quantification of tissue size (I), dorsal bristle number (J), and cell size (K). *P* values were calculated by one-way ANOVA. Error bars=S.D.; n=5. Genotypes: *ap-GAL4*/+ (A and G, Con in I to K), *ap-GAL4*/*dSesn*^{XP4} (B and H, *dSesn*^{XP4}

in I to K), *ap-GAL4 dSesn^{XP4}/dSesn^{XP4}* (C), *ap-GAL4/dSesn$^{XP4\Delta UAS}$* (D), *ap-GAL4/UAS-Myc-dSesn^{WT}* (E), *ap-GAL4/UAS-Myc-dSesn^{CS}* (F).

fig. S9. Expression of dSesn causes a reduction in compartment size by reducing cell size. Third instar larval wing imaginal discs of *ap-GAL4*/+ (*ap-GAL4*; A, C and E) and *ap-GAL4 dSesn^{XP4}/UAS-Myc-dSesn^{WT}* (*ap>2xdSesn*; B, D and F) flies were analyzed by staining with TRITC-phalloidin (Act, red), anti-Wingless (Wg, green) and DAPI (DAPI, blue). (**A** and **B**) Brackets indicate the approximate borders of the dorsal (D) and ventral (V) compartments. The dorsal compartment is reduced by two thirds (~67%) in *ap>2xdSesn* wing disc. (**C** to **F**) The dorsal areas in C and E include 79 cells, whereas the corresponding regions in D and F include 120 cells, indicating that cell size is reduced by two thirds (~66%) in the dorsal region of *ap>2xdSesn* wing disc. However the ventral areas of C and E show 91 cells and those of D and F show 89 cells, indicating that cell size in the ventral compartment remains largely unchanged (~102%) after *ap>2xdSesn* expression.

fig. S10. dSesn reduces ommatidia size without affecting photoreceptor cell number. (**A** to **F**) Scanning electron micrograph (SEM; A to D) and histology (E and F) of *gmr-GAL4/+* (A and C) and *gmr-GAL4/dSesn^{XP4}* (B and D) eyes. Lateral SEM images of whole eye (A and B) and magnified (C and D) views are presented. Histological sections were stained with toluidine blue to visualize photoreceptor cells. Scale bars, 100 μm (A), 10 μm (C and E). (**G**) Quantification of ommatidia sizes. Non-overlapping areas each

with 7 ommatidia in the central region of a SEM image were used for ommatidial size measurements. *P* values were calculated by one-way ANOVA. Error bars=S.D.; n=5. (**H**) Normal photoreceptor cell number per ommatidia (7) was unaffected by overexpression of dSesn (n>50).

fig. S11. dSesn reduces cell size by activating the AMPK-TSC module. (**A**) dSesn stimulates phosphorylation of TSC2 by AMPK. HEK293 cells were co-transfected with HA-AMPK along with GFP, mSesn2 or dSesn expression vectors. After 48 hrs, the cells were lysed and AMPK was immunoprecipitated and assayed for its ability to phosphorylate a TSC1:TSC2 complex that was isolated by immunoprecipitation from lysates of transiently transfected HEK293 cells. Phosphorylation of TSC2 was determined by incorporation of ^{32}P. The amounts of TSC2 in the assay mix and AMPK, mSesn2 and dSesn in the whole cell lysates (WCL) were examined by immunoblotting. (**B**) dSesn inhibits S6K phosphorylation. HEK293 cells were co-transfected with HA-S6K along with GFP, mSesn2 or dSesn expression vectors. After 48 hrs, HA-S6K was immunoprecipitated and its phosphorylation and total amount were examined by immunoblotting. mSesn2 and dSesn expression in total lysates was examined by immunoblotting. (**C**) TSC2 is required for inhibition of S6K phosphorylation upon dSesn expression. *Tsc2*$^{+/-}$, *Tsc2*$^{-/-}$ and Flag-TSC2-reconstituted *Tsc2*$^{-/-}$ MEFs were co-transfected with S6K together with dSesn or GFP expression vectors. HA-S6K was immunoprecipitated and its phosphorylation and expression were examined by immunoblotting. (**D** to **E**) Reduced TSC or AMPK activity attenuates the growth-

inhibitory effect of dSesn. Tissue size, cell size and cell number of a defined wing region bounded by L3, L4, C1 and extrapolated C2 veins in *ap-GAL4*/+ (Control), *ap-GAL4 dSesn*^{XP4}/+ (*ap>dSesn*), *ap-GAL4 dSesn*^{XP4}/+; *Tsc1*^{Q87X}/+ (*ap>dSesn Tsc1*$^{+/-}$), *ap-GAL4 dSesn*^{XP4}/+; *Tsc2*$^{E1.16}$/+ (*ap>dSesn Tsc2*$^{+/-}$), *ap-GAL4 dSesn*^{XP4}/*UAS-dAMPK*^{RNAi} (*ap>dSesn dAMPK*^{RNAi}), *ap-GAL4*/+; *Tsc1*^{Q87X}/+ (*ap-GAL4 Tsc1*$^{+/-}$), *ap-GAL4*/+; *Tsc2*$^{E1.16}$/+ (*ap-GAL4 Tsc2*$^{+/-}$), *ap-GAL4*/*UAS-dAMPK*^{RNAi} (*ap>dAMPK*^{RNAi}) flies were determined as in fig. S8. *P* values were calculated by one-way ANOVA. Error bars=S.D.; n=5. (**F**) siRNA-mediated silencing of AMPK by a *UAS-dAMPK*^{RNAi} transgene. After overnight egg collection, first instar larvae of *hs-GAL4*/+ (Control) and *UAS-dAMPK*^{RNAi}/+; *hs-GAL4*/+ (*hs>dAMPK*^{RNAi} or RNAi) flies were heat-shocked at 37°C for 1 hr and incubated at 25°C. Wandering-stage third instar larvae were collected and analyzed by quantitative RT-PCR for *AMPK* mRNA normalized to *rp49*. Error bars=S.D.; n=2. PCR products were analyzed by agarose gel electrophoresis and are shown in the inset.

fig. S12. Mammalian Sestrins inhibit cell growth in *Drosophila*. (**A** to **C**) Dorsal wing-specific expression of mSesn1 and mSesn2 causes the wings to bend upwards. (**D**) Eye-specific expression of mSesn1 and mSesn2 suppresses InR^{CA}-induced hyperplastic eye growth. Eye sizes were measured from frontal views of the different strains. *P* values were calculated by one-way ANOVA. Error bars=S.D.; n=3. Genotypes: *ap-GAL4*/+ (*ap-*Control), *ap-GAL4*/*UAS-Myc-mSesn1* (*ap>mSesn1*), *ap-GAL4*/*UAS-Myc-mSesn2* (*ap>mSesn2*), *gmr-GAL4 UAS-InR*^{CA}/+ (*gmr>InR*^{CA}), *gmr-GAL4 UAS-InR*^{CA}/*UAS-Myc-*

mSesn1 (*gmr>InR^{CA} mSesn1*), *gmr-GAL4 UAS-InR^{CA}/UAS-Myc-mSesn2* (*gmr>InR^{CA} mSesn2*).

fig. S13. Genetic interactions between dSesn and components of the TOR signaling pathway. Anterior views of wing blades with *ap*-driven expression of the indicated genetic elements. The dorsal side is placed upwards. (**A** to **H**) dSesn suppresses the downward bending of the wings induced by wing-specific expression of InR-, PI3K^{CA}- and AKT-, but not S6K^{CA}. (**I** to **P**) dSesn enhances the upward bending of the wings that is induced by wing-specific expression of InR^{DN}-, PI3K^{DN}-, PTEN- and S6K^{DN}. Genotypes: *ap-GAL4*/*UAS-InR* (A), *UAS-PI3K^{CA}*/Y; *ap-GAL4*/+ (B), *ap-GAL4*/*UAS-AKT* (C), *ap-GAL4*/*UAS-S6k^{CA}* (D), *ap-GAL4 dSesn^{XP4}*/*UAS-InR* (E), *UAS-PI3K^{CA}*/Y; *ap-GAL4 dSesn^{XP4}*/+ (F), *ap-GAL4 dSesn^{XP4}*/*UAS-AKT* (G), *ap-GAL4 dSesn^{XP4}*/*UAS-S6k^{CA}* (H), *ap-GAL4*/*UAS-InR^{DN}* (I), *UAS-PI3K^{DN}*/Y; *ap-GAL4*/+ (J), *ap-GAL4*/*UAS-Pten* (K), *ap-GAL4*/*UAS-S6k^{DN}* (L), *ap-GAL4 dSesn^{XP4}*/*UAS-InR^{DN}* (M), *UAS-PI3K^{DN}*/Y; *ap-GAL4 dSesn^{XP4}*/+ (N), *ap-GAL4 dSesn^{XP4}*/*UAS-Pten* (O), *ap-GAL4 dSesn^{XP4}*/*UAS-S6k^{DN}* (P).

fig. S14. Role of endogenous dSesn in TOR signaling. (**A** to **J**) Anterior views of wing blades with *ap*-driven expression of the indicated genetic elements in wild-type or *dSesn*-null (*dSesn$^{-/-}$*) backgrounds. *UAS-InR^{CA}* induced wing overgrowth and downward bending in *dSesn*-null background, even in the absence of the Gal4 driver. The dorsal side is placed upwards. Genotypes: *UAS-InR^{CA}* (A), *UAS-InR^{CA} dSesn^{8A11}*/ *UAS-InR^{CA} dSesn^{8A11}* (B), *ap-GAL4*/*UAS-S6k* (C), *ap-GAL4 dSesn^{8A11}*/*UAS-S6k dSesn^{8A11}* (D), *ap-GAL4*/*UAS-*

S6k^{CA} (E), *ap-GAL4 dSesn*^{8A11}/*UAS-S6k*^{CA} *dSesn*^{8A11} (F), *ap-GAL4*/*UAS-InR*^{DN} (G), *ap-GAL4 dSesn*^{8A11}/*UAS-InR*^{DN} *dSesn*^{8A11} (H), *ap-GAL4*/*UAS-S6k*^{DN} (I), *ap-GAL4 dSesn*^{8A11}/*UAS-S6k*^{DN} *dSesn*^{8A11} (J).

fig. S15. *dSesn*-null mutants accumulate more triglycerides. Total triglycerides were measured in five 10-day-old adult males of WT (*dSesn*$^{+/+}$), *dSesn*^{8A11}/*dSesn*^{8A11} (*dSesn*^{8A11}), and *dSesn*^{8A11}/*dSesn*^{3F6} (*dSesn*$^{8A11/3F6}$). *P* values were calculated by one-way ANOVA. Error bars=S.D.; n=3.

fig. S16. Cardiac phenotypes of *dSesn*-null flies. (**A**) Diastolic and systolic intervals (seconds) were measured in the flies described in Fig. 5, and are shown as bar graphs. Error bars indicate S.E.M.; n>10. (**B**) Diastolic and systolic diameters (μm) were measured in the flies described in Fig. 5, and are shown as bar graphs. *P* values were calculated using one-way ANOVA between WT and *dSesn*$^{-/-}$. Error bars indicate S.E.M.; n>10.

fig. S17. Cardiac malfunction caused by heart-specific silencing of dSesn and dAMPK. (**A** to **C**) Representative M mode records of 2-week-old *hand-GAL4/+*; *hand-GAL4 UAS-GFP/+* (*hand-GFP*), *hand-GAL4/+*; *hand-GAL4 UAS-GFP/UAS-dSesn*^{RNAi} (*hand>dSesn*^{RNAi}) and *hand-GAL4/UAS-dAMPK*^{RNAi}; *hand-GAL4 UAS-GFP/+* (*hand>dAMPK*^{RNAi}) adult flies, showing the movement of heart tube walls (y-axis) over time (x-axis). 1 second is indicated by the bar. (**D** and **E**) Quantification of cardiac

function parameters. *P* values were calculated using one-way ANOVA. Error bars indicate S.E.M.; n≥19. (**F**) Efficiency of *UAS-dSesn*^{RNAi}-mediated silencing. Lysates of *UAS-Dcr2*/Y; *Act-GAL4*/+ (*Act-GAL4*) and *UAS-Dcr2*/Y; *Act-GAL4*/+; *UAS-dSesn*^{RNAi}/+ (*Act>dSesn*^{RNAi}) adult male flies were analyzed by immunoblotting with anti-dSesn and anti-tubulin antibodies. (**G**) RNAs purified from adult hearts of *hand-GAL4/+*; *hand-GAL4 UAS-GFP/+* (*hand>GFP*) or *hand-GAL4/+*; *hand-GAL4 UAS-GFP/UAS-dSesn*^{RNAi} (*hand>dSesn*^{RNAi}) flies were analyzed by quantitative RT-PCR to examine the amounts of dSesn mRNA that were normalized to the amounts of rp49 mRNA. Error bars=S.D.; n=4.

fig. S18. dSesn is abundantly expressed in muscle-enriched tissues. (**A**) Northern blot analyses of adult and larval tissues. The indicated tissues were isolated from 10-days-old adults or third instar larvae, and subjected to Northern blot analyses with the indicated probes. Tissues showing high levels of dSesn expression (adult thorax, larval epidermis and gut) contain muscles. (**B**) Immunoblot analysis of adult tissues, demonstrating high amounts of dSesn protein in the thorax, which is mainly composed of indirect flight muscles. Lysates of the indicated tissues were immunoblotted with anti-dSesn and anti-tubulin (Tub) antibodies. Note that the "Total" lane is the same one as the first lane in fig. S4C, where it is labeled *dSesn*$^{+/+}$.

fig. S19. Loss of dSesn results in progressive muscle degeneration. Thoracic skeletal muscles of 20-day-old *dSesn*$^{\delta A11}$/+ (**A** to **D**), 20-day-old (**E** to **H**) and 5-day-old (**I** to **L**)

dSesn^{8A11}/*dSesn*^{3F6} adult flies were analyzed by TEM. *, Z-discs; **, M-band. First column, transverse sections shown in low magnification; Second column, tilted longitudinal sections shown in low magnification; Third column, transverse sections of actomyosin bundles shown in high magnification; Fourth column, internal structures of mitochondria shown in high magnification. Scale bars, 1 μm (first and second column), 0.1 μm (third and fourth column).

fig. S20. Accumulation of ROS and polyubiquitin aggregates and cell death in *dSesn*-null muscles. (**A**, **C**, and **D**) Indirect flight muscles from 10-day-old *w*^{1118} (WT) and *dSesn*^{8A11} (*dSesn*$^{-/-}$) male flies were analyzed for ROS accumulation (by DHE staining), presence of apoptotic cells (by TUNEL staining), and presence of polyubiquitin aggregates (by staining with anti-ubiquitin antibody). (**B**) Total *cis*-aconitase activity in 10-day-old *w*^{1118} (WT) and *dSesn*^{8A11} (*dSesn*$^{-/-}$) adult male flies was measured as described in Materials and Methods. The isocitrate produced by *cis*-aconitase was converted by isocitrate dehydrogenase in presence of NADP, Fe^{2+}, MTT and PMS to a chromogenic product.

fig. S21. Reduced dAMPK or dATG1 expression in skeletal muscle results in muscle degeneration. Thoracic skeletal muscles of 10-day-old *UAS-Dcr2*/Y; *Mef2-GAL4*/+ (**A** to **D**), 1-day-old *UAS-Dcr2*/+; *Mef2-GAL4/UAS-dAMPK*^{RNAi} (**E** to **H**), 10-day-old *UAS-Dcr2*/+; *Mef2-GAL4*/+; *UAS-dATG1*^{RNAi}/+ (**I** to **L**) and 10-day-old *Thor*^{1} (**M** to **P**) adult flies were analyzed by TEM. All *UAS-Dcr2*/+; *Mef2-GAL4/UAS-dAMPK*^{RNAi} adult flies died within one day after eclosion. *UAS-Dcr2*/Y; *Mef2-GAL4/UAS-dAMPK*^{RNAi} and *UAS-*

*Dcr2/*Y; *Mef2-GAL4/*+; *UAS-dATG1*^{RNAi}/+ flies failed to develop into adulthood. First column, transverse sections shown in low magnification; Second column, tilted longitudinal sections shown in low magnification; Third column, transverse sections of actomyosin bundles shown in high magnification; Fourth column, internal structures of mitochondria shown in high magnification. Scale bars, 1 μm (first and second column), 0.1 μm (third and fourth column).

References for Supporting Online Material

1. M. D. Adams *et al.*, *Science* **287**, 2185 (2000).
2. S. T. Thibault *et al.*, *Nat Genet* **36**, 283 (2004).
3. A. V. Budanov, A. A. Sablina, E. Feinstein, E. V. Koonin, P. M. Chumakov, *Science* **304**, 596 (2004).
4. A. H. Brand, N. Perrimon, *Development* **118**, 401 (1993).
5. D. C. Goberdhan, N. Paricio, E. C. Goodman, M. Mlodzik, C. Wilson, *Genes Dev* **13**, 3244 (1999).
6. S. Wu, J. Huang, J. Dong, D. Pan, *Cell* **114**, 445 (2003).
7. N. Tapon, N. Ito, B. J. Dickson, J. E. Treisman, I. K. Hariharan, *Cell* **105**, 345 (2001).
8. K. F. Harvey *et al.*, *J Cell Biol* **180**, 691 (2008).
9. M. A. Junger *et al.*, *J Biol* **2**, 20 (2003).
10. Z. Han, P. Yi, X. Li, E. N. Olson, *Development* **133**, 1175 (2006).
11. G. Dietzl *et al.*, *Nature* **448**, 151 (2007).
12. H. Nagaso, T. Murata, N. Day, K. K. Yokoyama, *J Histochem Cytochem* **49**, 1177 (2001).
13. E. Owusu-Ansah, A. Yavari, S. Mandal, U. Banerjee, *Nat Genet* **40**, 356 (2008).
14. W. Zheng, S. Ren, J. H. Graziano, *Brain Res* **799**, 334 (1998).
15. A. V. Budanov, M. Karin, *Cell* **134**, 451 (2008).
16. I. Y. Dobrosotskaya, A. C. Seegmiller, M. S. Brown, J. L. Goldstein, R. B.

Rawson, *Science* **296**, 879 (2002).

17. N. Luong *et al.*, *Cell Metab* **4**, 133 (2006).

18. P. Vigne, M. Tauc, C. Frelin, *PLoS One* **4**, e5422 (2009).

19. C. Driver, A. Georgeou, *Biogerontology* **4**, 91 (2003).

20. K. A. Ocorr, T. Crawley, G. Gibson, R. Bodmer, *PLoS One* **2**, e601 (2007).

21. R. Wessells *et al.*, *Aging Cell* **8**, 542 (2009).

22. T. Furuyama, T. Nakazawa, I. Nakano, N. Mori, *Biochem J* **349**, 629 (2000).

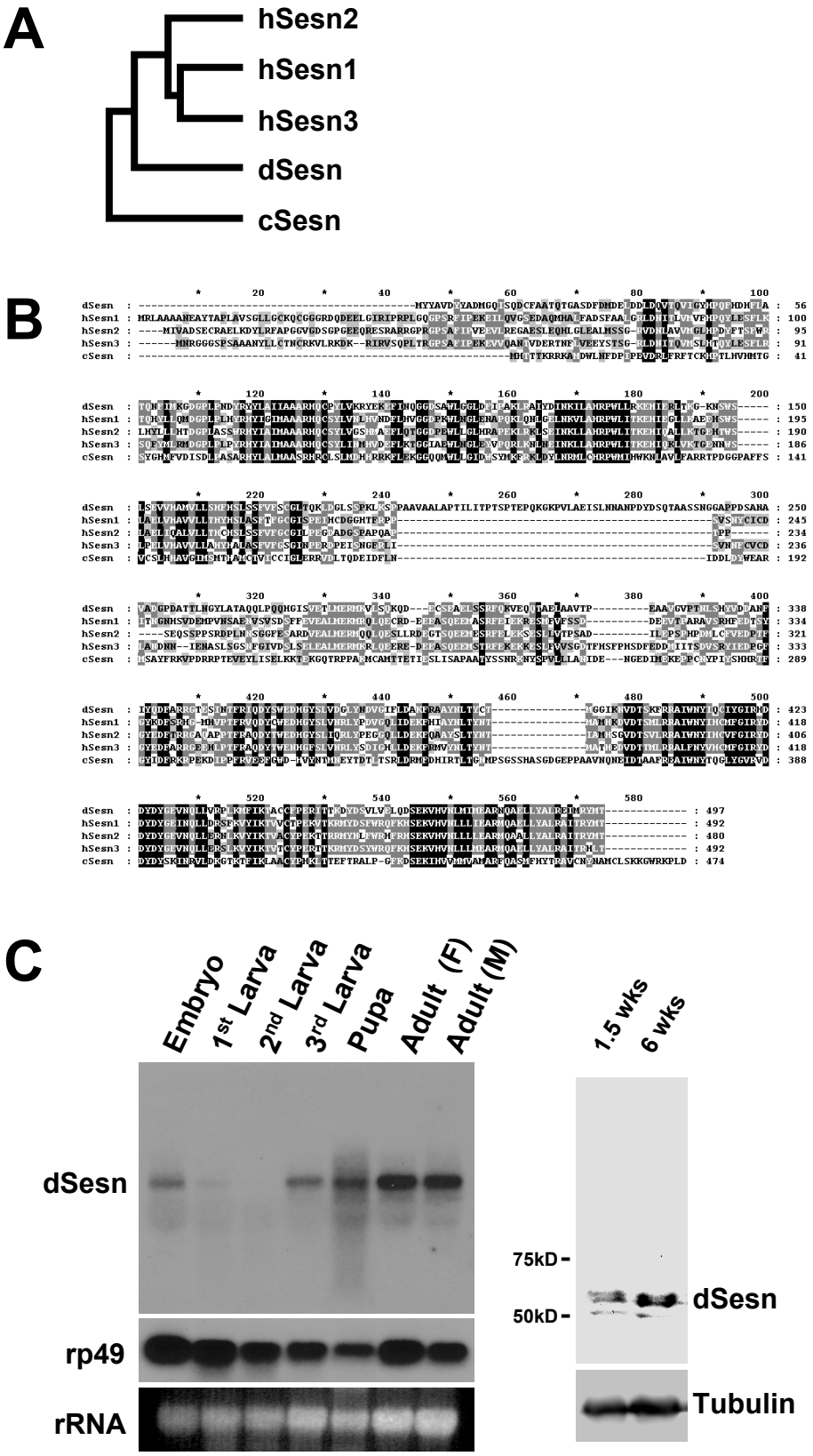
A
hSesn2
hSesn1
hSesn3
dSesn
cSesn
B
C
Embryo
1st Larva
2nd Larva
3rd Larva
Pupa
Adult (F)
Adult (M)
1.5 wks
6 wks
dSesn
rp49
rRNA
75kD
50kD
dSesn
Tubulin

Fig. S1

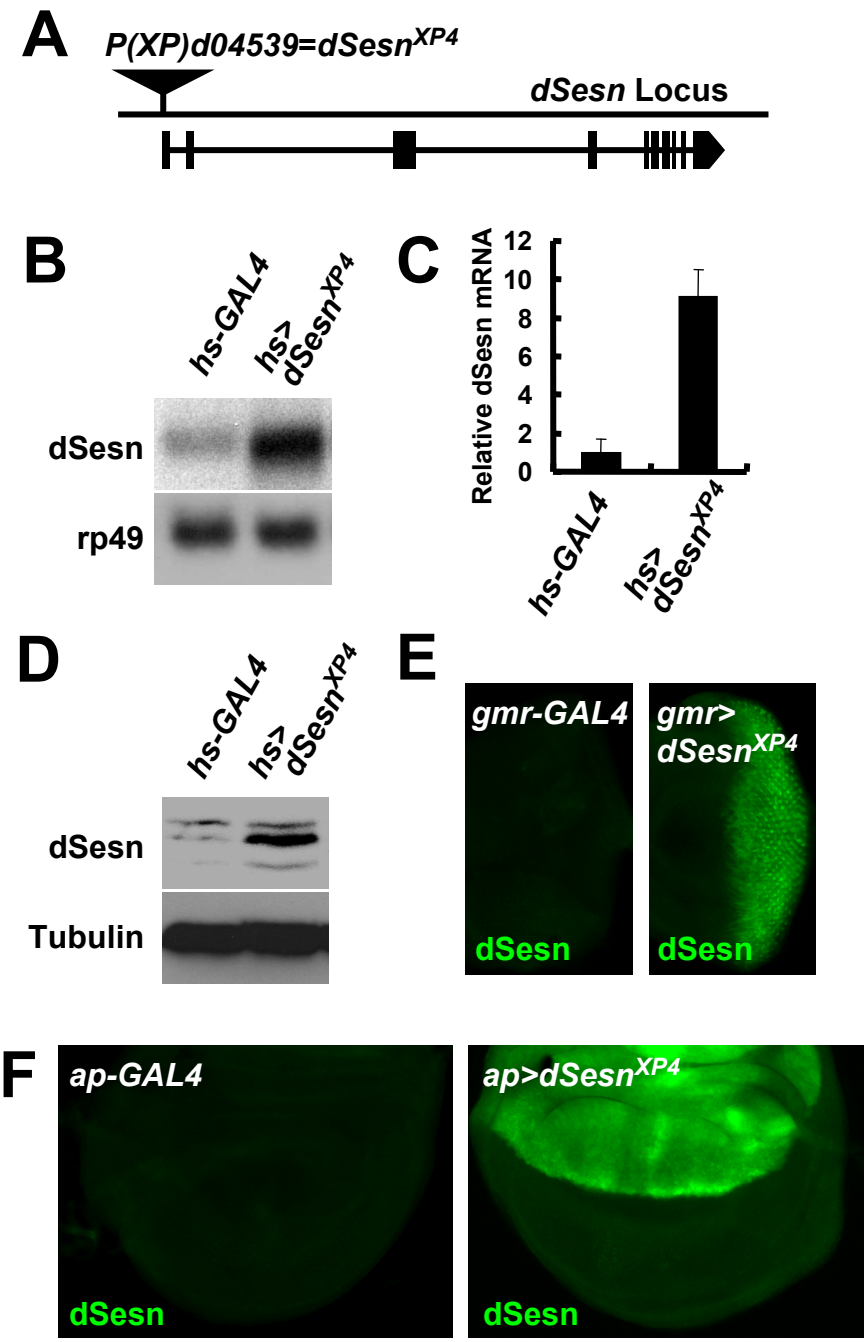
A
P(XP)d04539=dSesn^XP4
dSesn Locus
B
hs-GAL4
hs> dSesn^XP4
dSesn
rp49
C
Relative dSesn mRNA
12
10
8
6
4
2
0
hs-GAL4
hs> dSesn^XP4
D
hs-GAL4
hs> dSesn^XP4
dSesn
Tubulin
E
gmr-GAL4
dSesn
gmr> dSesn^XP4
dSesn
F
ap-GAL4
dSesn
ap>dSesn^XP4
dSesn

Fig. S2

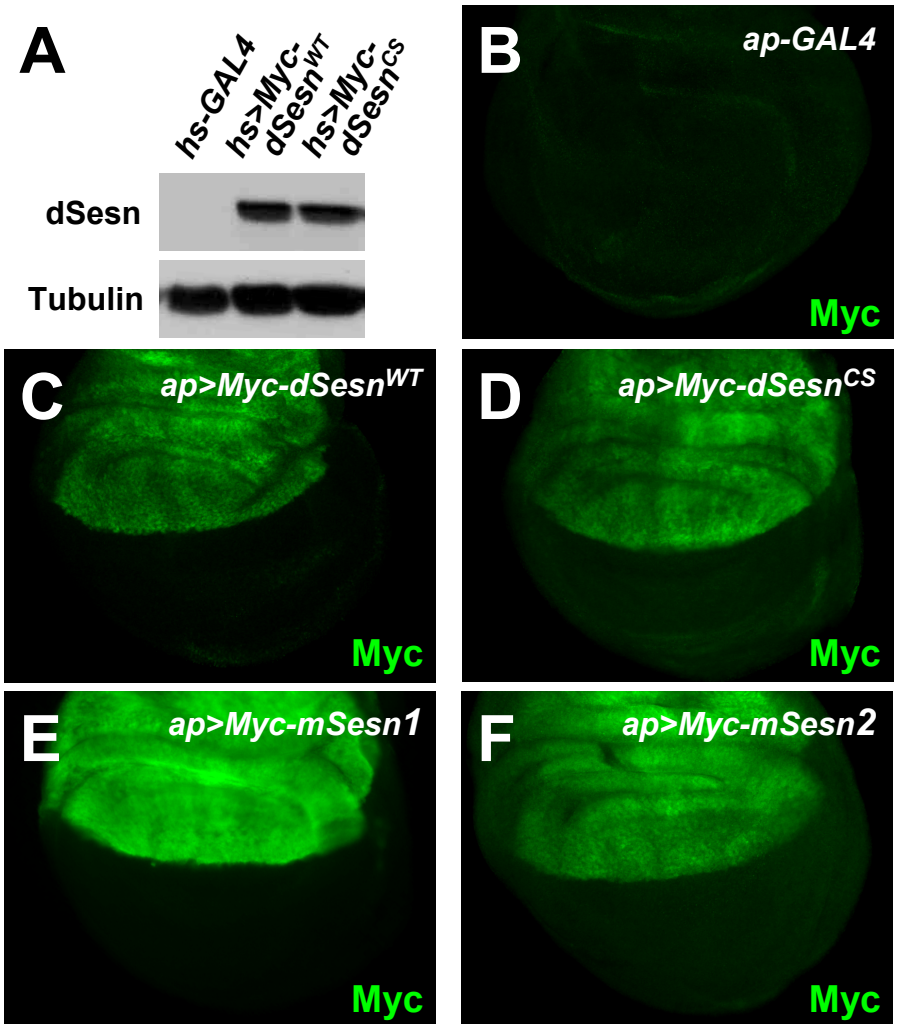
A
hs-GAL4
hs>Myc-dSesn^WT
hs>Myc-dSesn^CS
dSesn
Tubulin
B
ap-GAL4
Myc
C
ap>Myc-dSesn^WT
Myc
D
ap>Myc-dSesn^CS
Myc
E
ap>Myc-mSesn1
Myc
F
ap>Myc-mSesn2
Myc

Fig. S3

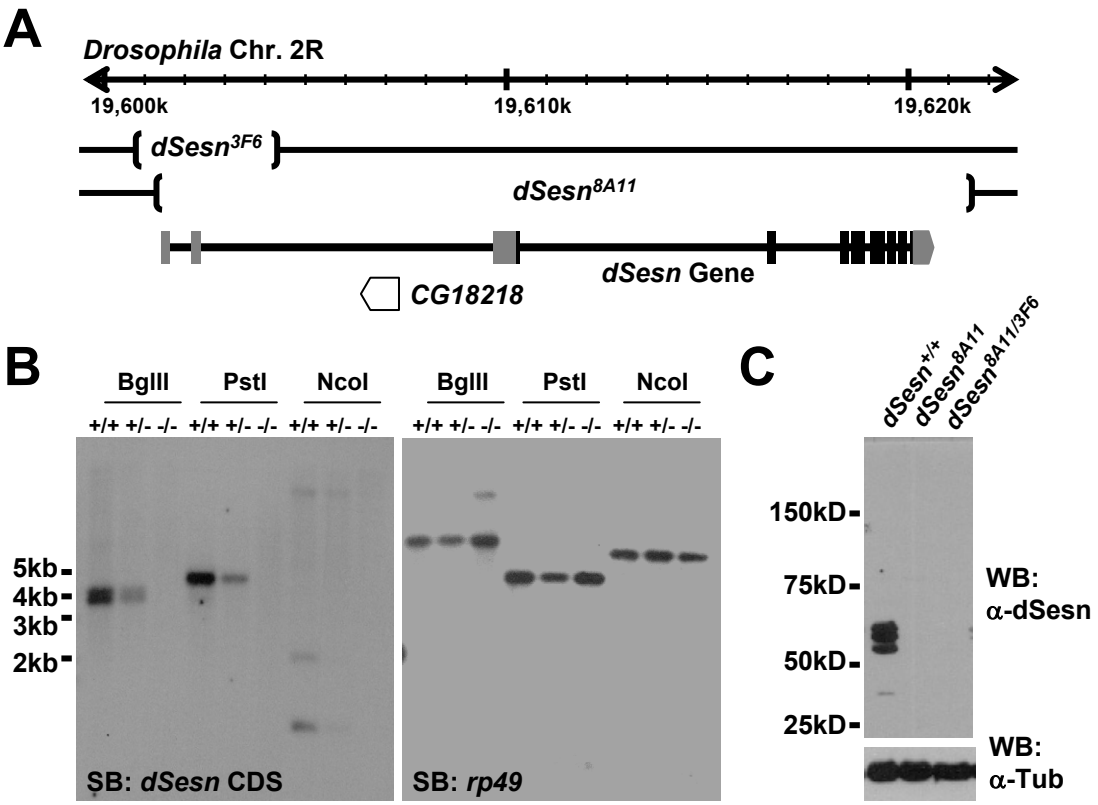
A
Drosophila Chr. 2R
19,600k
19,610k
19,620k
dSesn3F6
dSesn8A11
dSesn Gene
CG18218
B
BglII
PstI
NcoI
BglII
PstI
NcoI
+/+ +/- -/- +/+ +/- -/- +/+ +/- -/-
+/+ +/- -/- +/+ +/- -/- +/+ +/- -/-
5kb
4kb
3kb
2kb
SB: dSesn CDS
SB: rp49
C
dSesn+/+
dSesn8A11
dSesn8A11/3F6
150kD
75kD
50kD
25kD
WB:
α-dSesn
WB:
α-Tub

Fig. S4

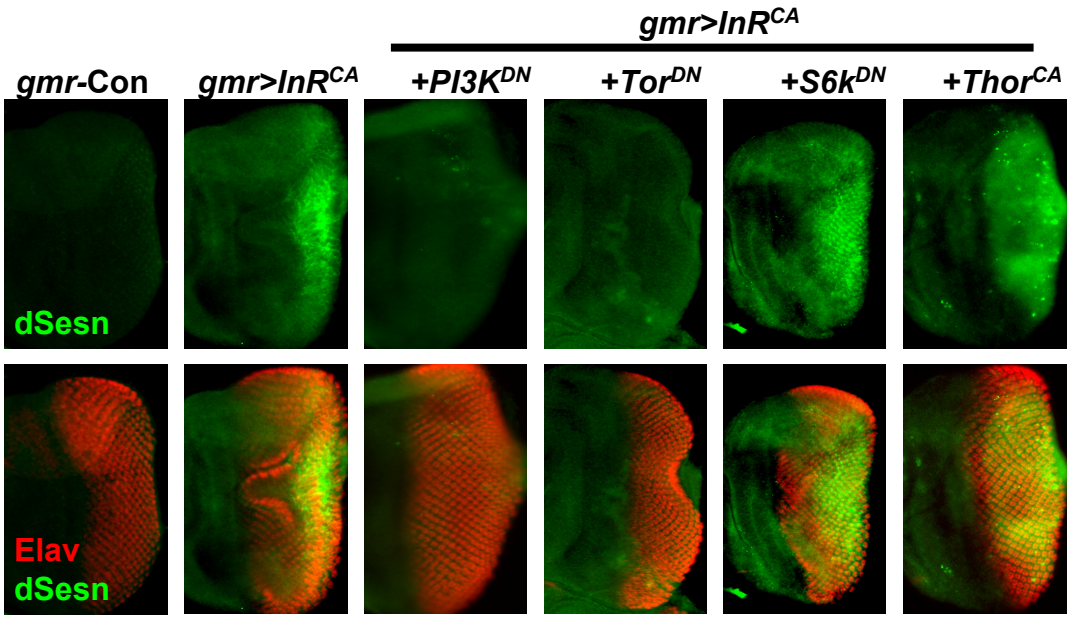
gmr>InR^CA
gmr-Con
gmr>InR^CA
+PI3K^DN
+Tor^DN
+S6k^DN
+Thor^CA
dSesn
Elav
dSesn

Fig. S5

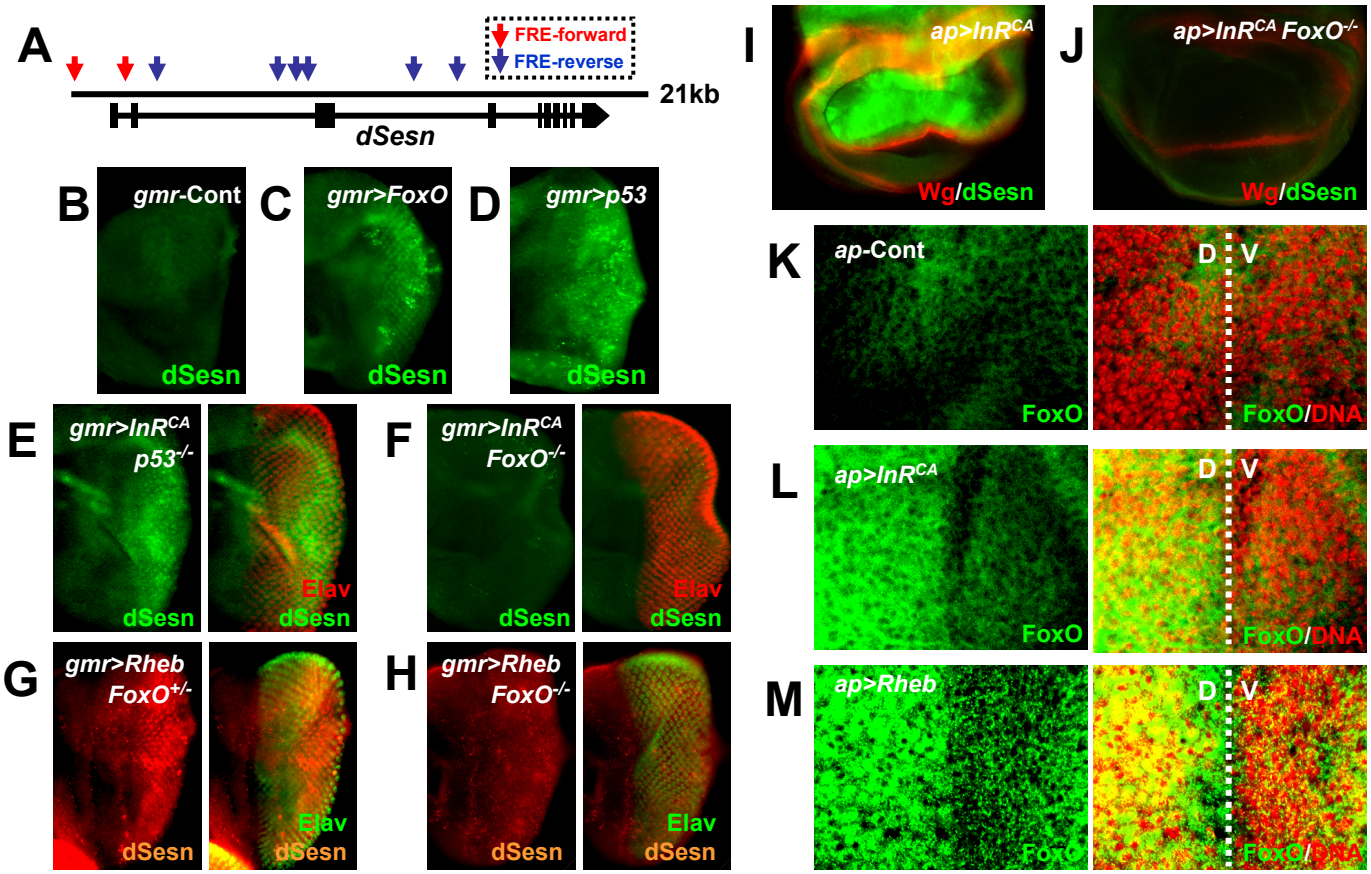
A
FRE-forward
FRE-reverse
21kb
dSesn
B
gmr-Cont
dSesn
C
gmr>FoxO
dSesn
D
gmr>p53
dSesn
E
gmr>InR^CA p53^-/-
dSesn
Elav
dSesn
F
gmr>InR^CA FoxO^-/-
dSesn
Elav
dSesn
G
gmr>Rheb FoxO^+/-
dSesn
Elav
dSesn
H
gmr>Rheb FoxO^-/-
dSesn
Elav
dSesn
I
ap>InR^CA
Wg/dSesn
J
ap>InR^CA FoxO^-/-
Wg/dSesn
K
ap-Cont
FoxO
D
V
FoxO/DNA
L
ap>InR^CA
FoxO
D
V
FoxO/DNA
M
ap>Rheb
FoxO
D
V
FoxO/DNA

Fig. S6

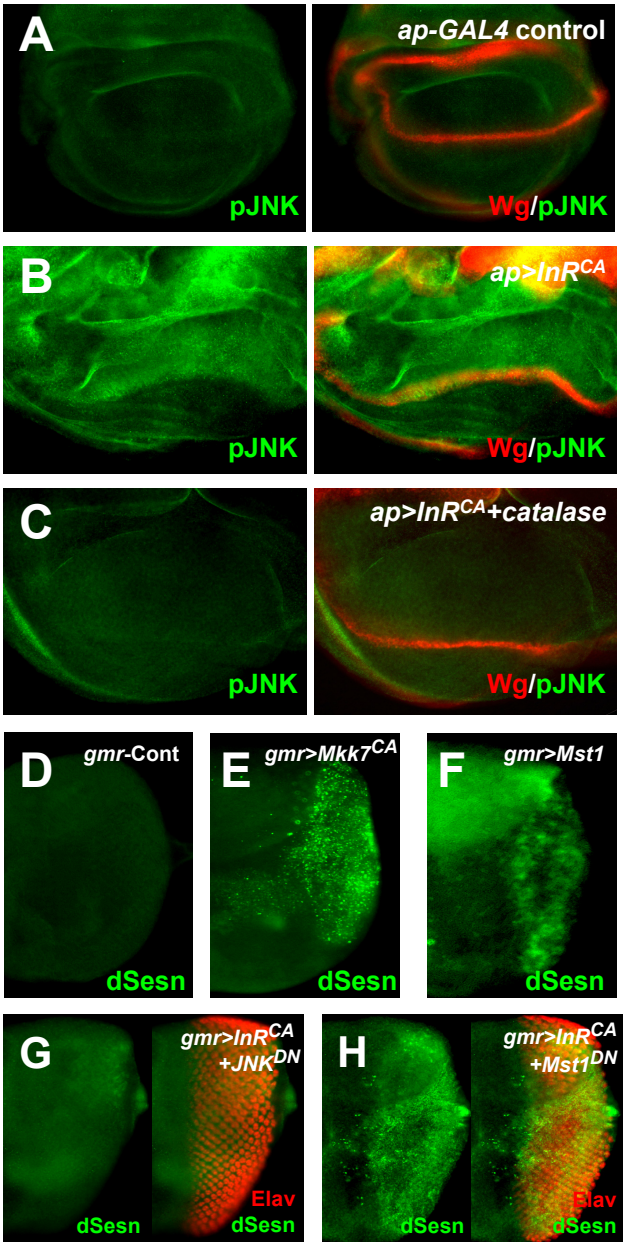
A
ap-GAL4 control
pJNK
Wg/pJNK
B
ap>InR^CA
pJNK
Wg/pJNK
C
ap>InR^CA+catalase
pJNK
Wg/pJNK
D
gmr-Cont
dSesn
E
gmr>Mkk7^CA
dSesn
F
gmr>Mst1
dSesn
G
gmr>InR^CA +JNK^DN
dSesn
Elav
dSesn
H
gmr>InR^CA +Mst1^DN
dSesn
Elav
dSesn

Fig. S7

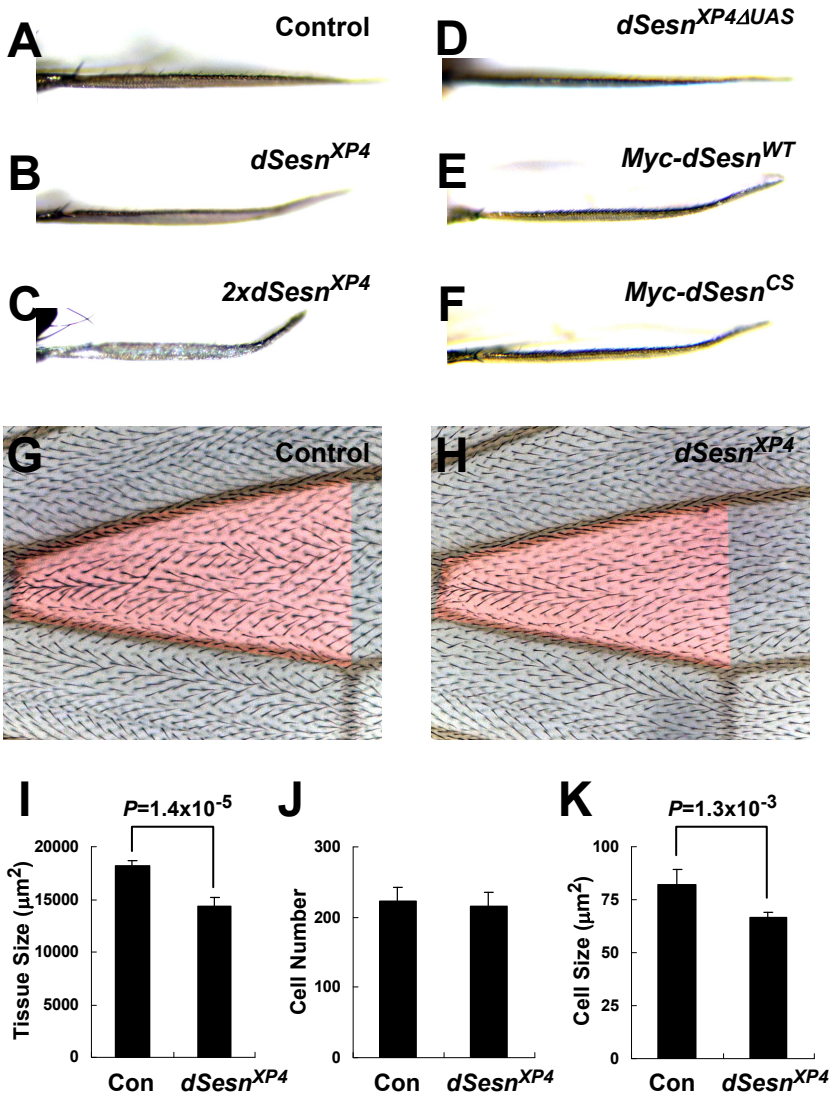
A
Control
B
dSesn^XP4
C
2xdSesn^XP4
D
dSesn^XP4ΔUAS
E
Myc-dSesn^WT
F
Myc-dSesn^CS
G
Control
H
dSesn^XP4
I
P=1.4x10^-5
Tissue Size (μm^2)
20000
15000
10000
5000
0
Con
dSesn^XP4
J
Cell Number
300
200
100
0
Con
dSesn^XP4
K
P=1.3x10^-3
Cell Size (μm^2)
100
75
50
25
0
Con
dSesn^XP4

Fig. S8

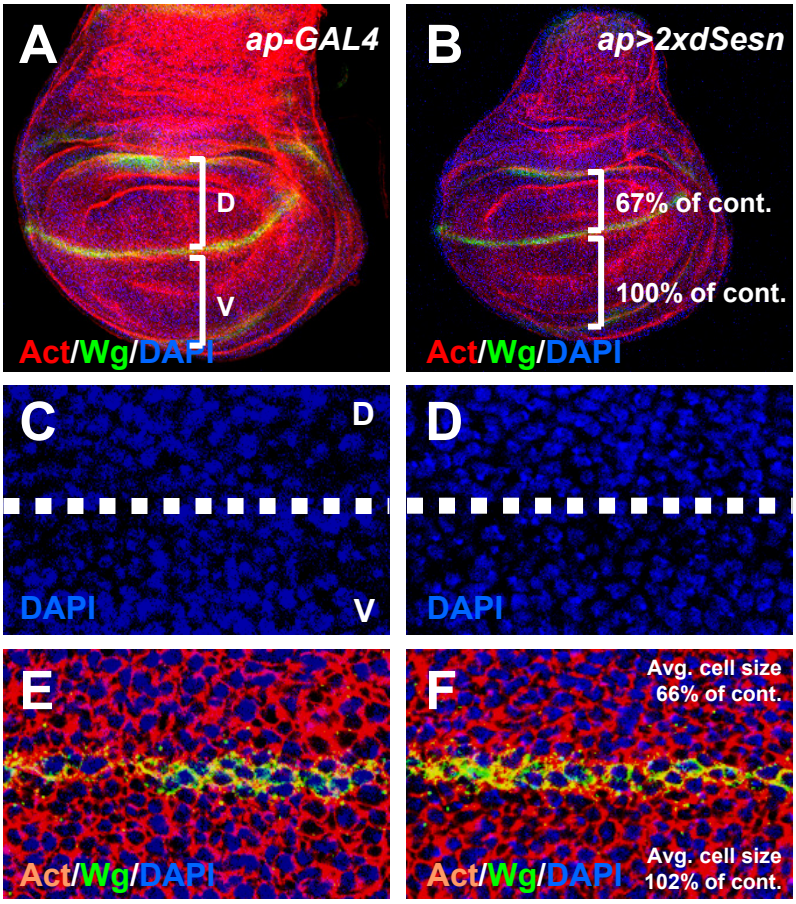
A
ap-GAL4
D
V
Act/Wg/DAPI
B
ap>2xdSesn
67% of cont.
100% of cont.
Act/Wg/DAPI
C
D
DAPI
V
D
DAPI
E
Act/Wg/DAPI
F
Avg. cell size
66% of cont.
Act/Wg/DAPI
Avg. cell size
102% of cont.

Fig. S9

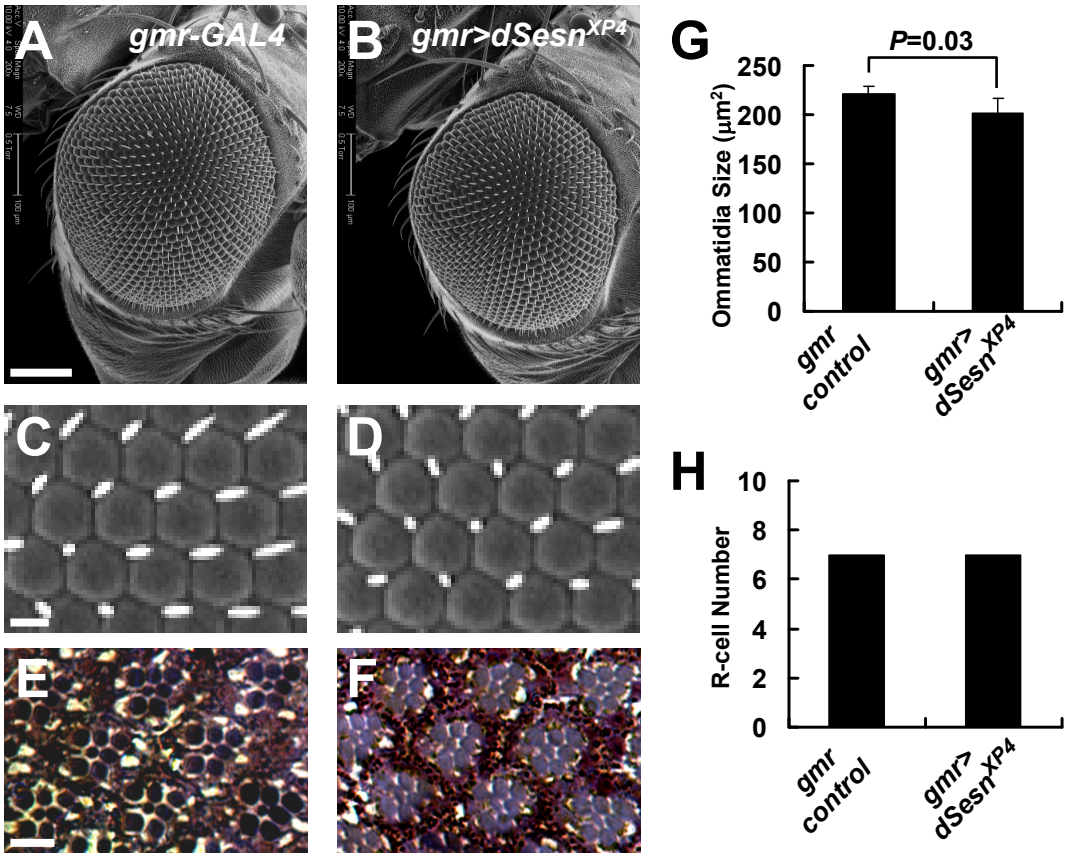
A
gmr-GAL4
B
gmr>dSesn^XP4
C
D
E
F
G
P=0.03
Ommatidia Size (μm²)
250
200
150
100
50
0
gmr control
gmr> dSesn^XP4
H
R-cell Number
10
8
6
4
2
0
gmr control
gmr> dSesn^XP4

Fig. S10

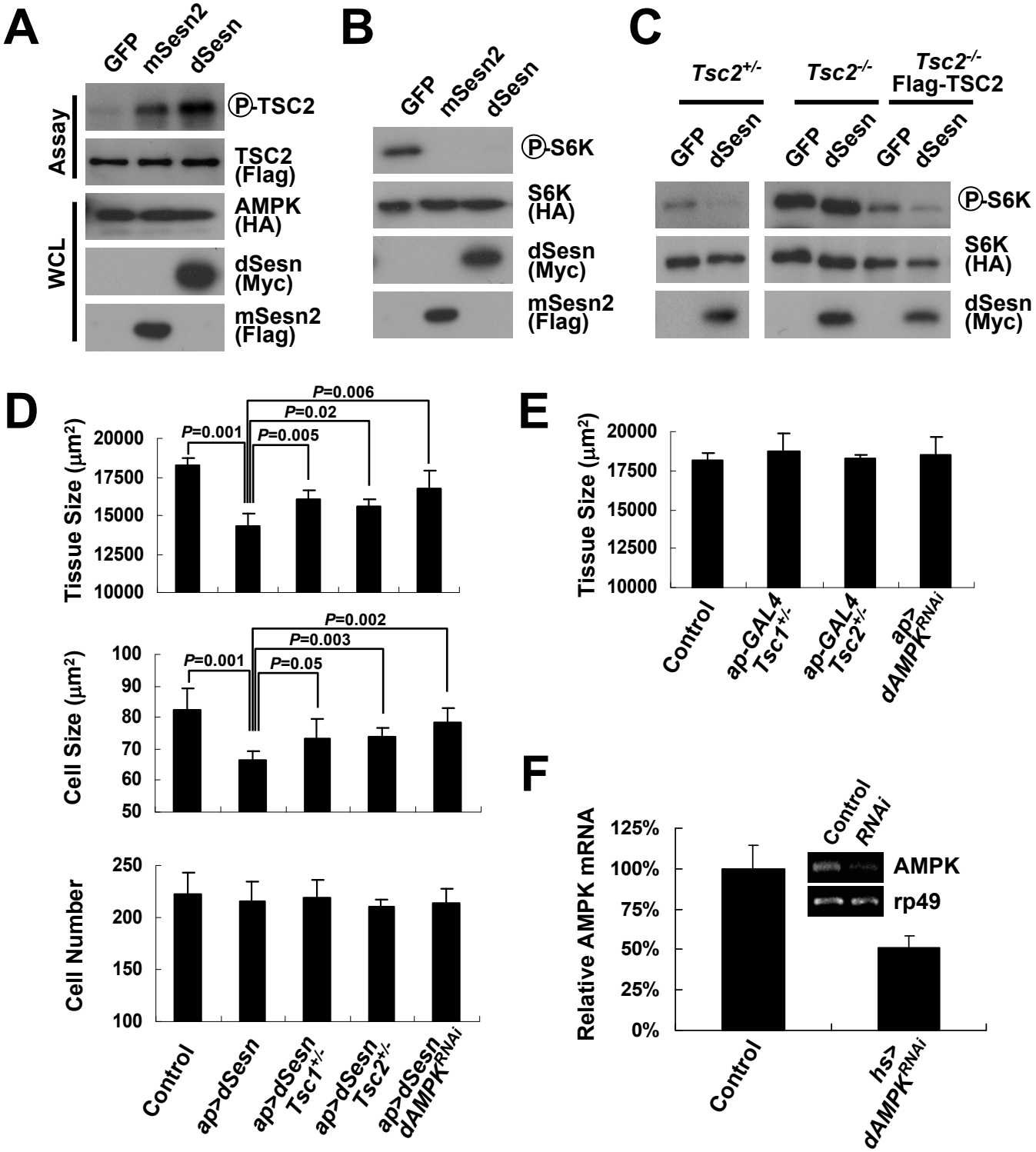
A
GFP
mSesn2
dSesn
Assay
WCL
Ⓟ-TSC2
TSC2 (Flag)
AMPK (HA)
dSesn (Myc)
mSesn2 (Flag)
B
GFP
mSesn2
dSesn
Ⓟ-S6K
S6K (HA)
dSesn (Myc)
mSesn2 (Flag)
C
Tsc2+/-
Tsc2-/-
Tsc2-/- Flag-TSC2
GFP
dSesn
Ⓟ-S6K
S6K (HA)
dSesn (Myc)
D
Tissue Size (μm2)
P=0.001
P=0.005
P=0.02
P=0.006
Cell Size (μm2)
P=0.001
P=0.05
P=0.003
P=0.002
Cell Number
Control
ap>dSesn
ap>dSesn Tsc1+/-
ap>dSesn Tsc2+/-
ap>dSesn dAMPKRNAi
E
Tissue Size (μm2)
Control
ap-GAL4 Tsc1+/-
ap-GAL4 Tsc2+/-
ap> dAMPKRNAi
F
Relative AMPK mRNA
Control RNAi
AMPK
rp49
Control
hs> dAMPKRNAi

Fig. S11

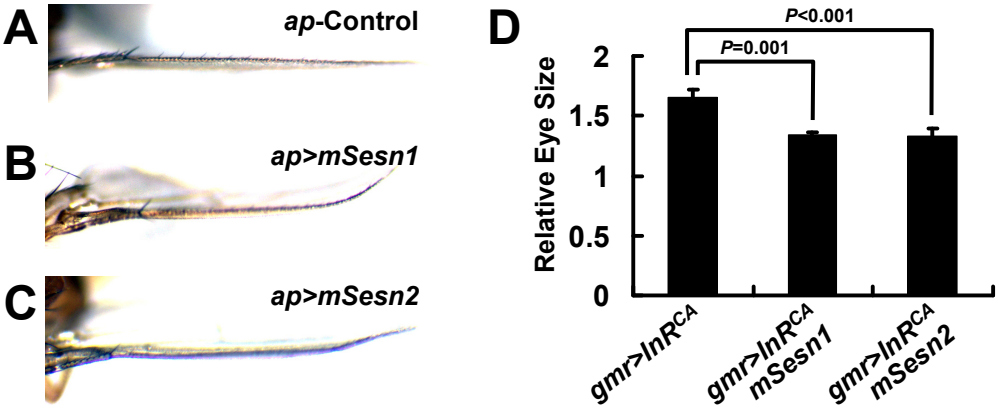
A
ap-Control
B
ap>mSesn1
C
ap>mSesn2
D
P<0.001
P=0.001
Relative Eye Size
2
1.5
1
0.5
0
gmr>InR^CA
gmr>InR^CA mSesn1
gmr>InR^CA mSesn2

Fig. S12

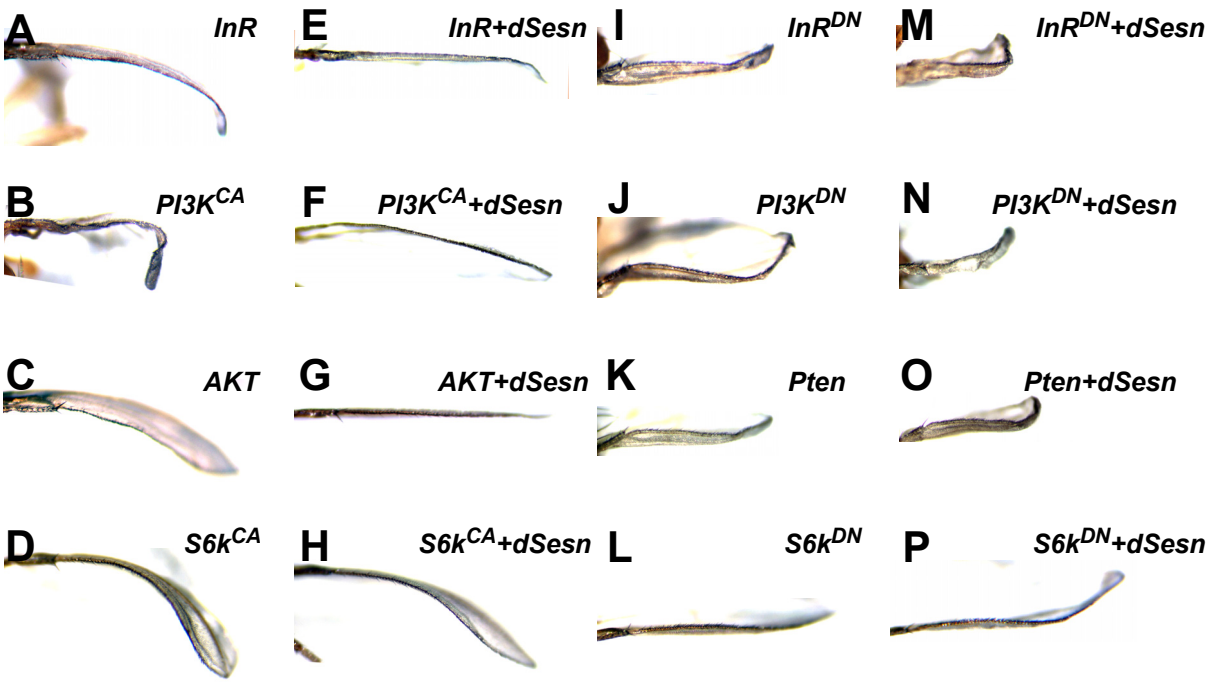
A
InR
E
InR+dSesn
I
InR^DN
M
InR^DN+dSesn
B
PI3K^CA
F
PI3K^CA+dSesn
J
PI3K^DN
N
PI3K^DN+dSesn
C
AKT
G
AKT+dSesn
K
Pten
O
Pten+dSesn
D
S6k^CA
H
S6k^CA+dSesn
L
S6k^DN
P
S6k^DN+dSesn

Fig. S13

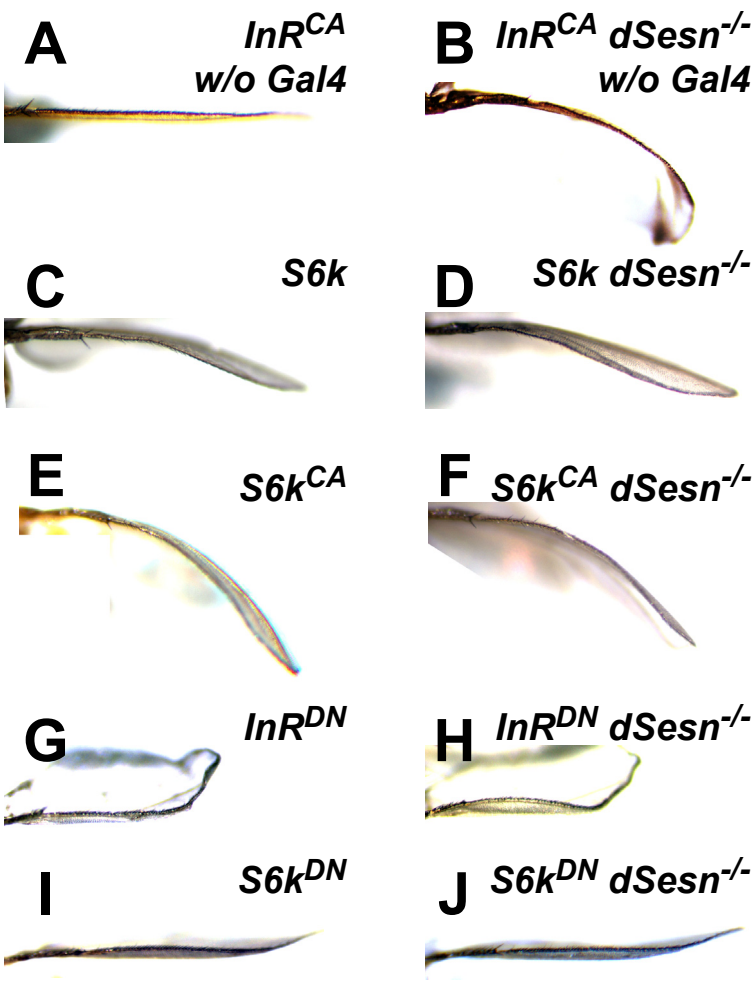
A
InR^CA
w/o Gal4
B
InR^CA dSesn^-/-
w/o Gal4
C
S6k
D
S6k dSesn^-/-
E
S6k^CA
F
S6k^CA dSesn^-/-
G
InR^DN
H
InR^DN dSesn^-/-
I
S6k^DN
J
S6k^DN dSesn^-/-

Fig. S14

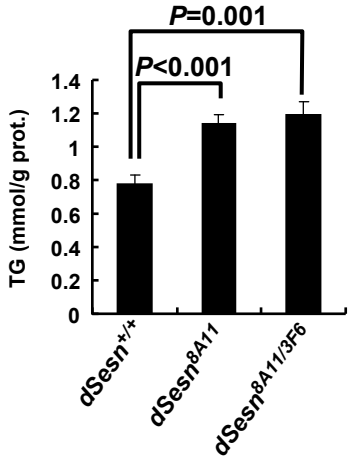
P=0.001
P<0.001
TG (mmol/g prot.)
1.4
1.2
1
0.8
0.6
0.4
0.2
0
dSesn+/+
dSesn8A11
dSesn8A11/3F6

Fig. S15

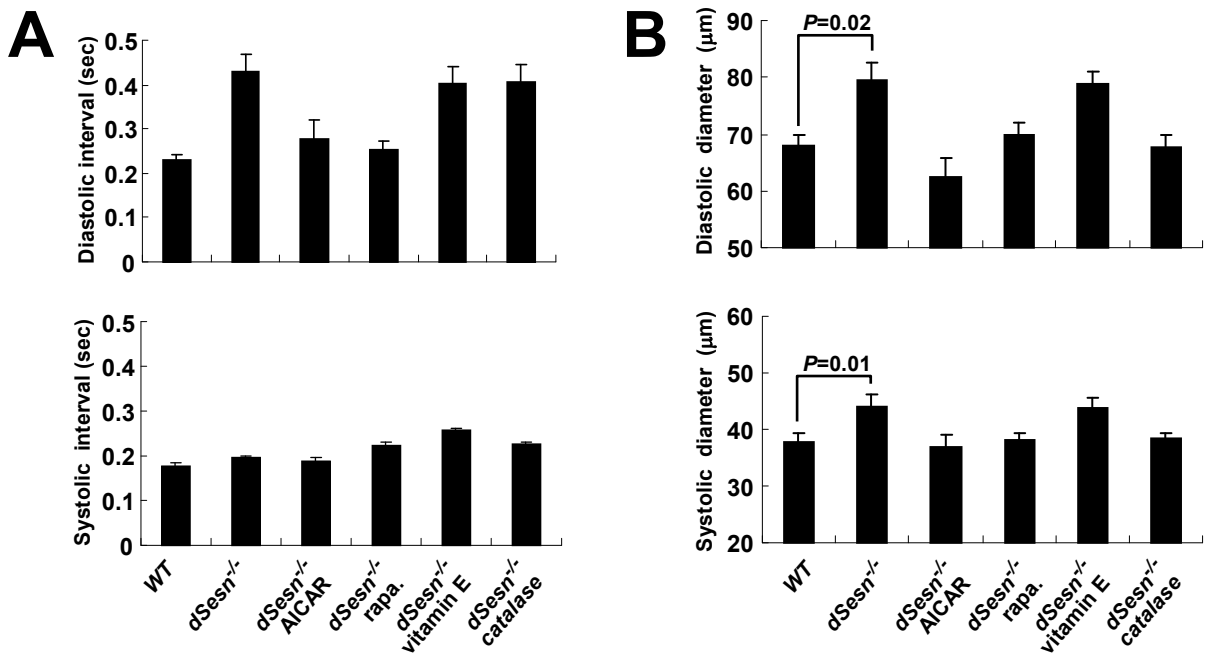
A
Diastolic interval (sec)
0
0.1
0.2
0.3
0.4
0.5
Systolic interval (sec)
0
0.1
0.2
0.3
0.4
0.5
WT
dSesn-/-
dSesn-/- AICAR
dSesn-/- rapa.
dSesn-/- vitamin E
dSesn-/- catalase
B
Diastolic diameter (μm)
50
60
70
80
90
P=0.02
Systolic diameter (μm)
20
30
40
50
60
P=0.01
WT
dSesn-/-
dSesn-/- AICAR
dSesn-/- rapa.
dSesn-/- vitamin E
dSesn-/- catalase

Fig. S16

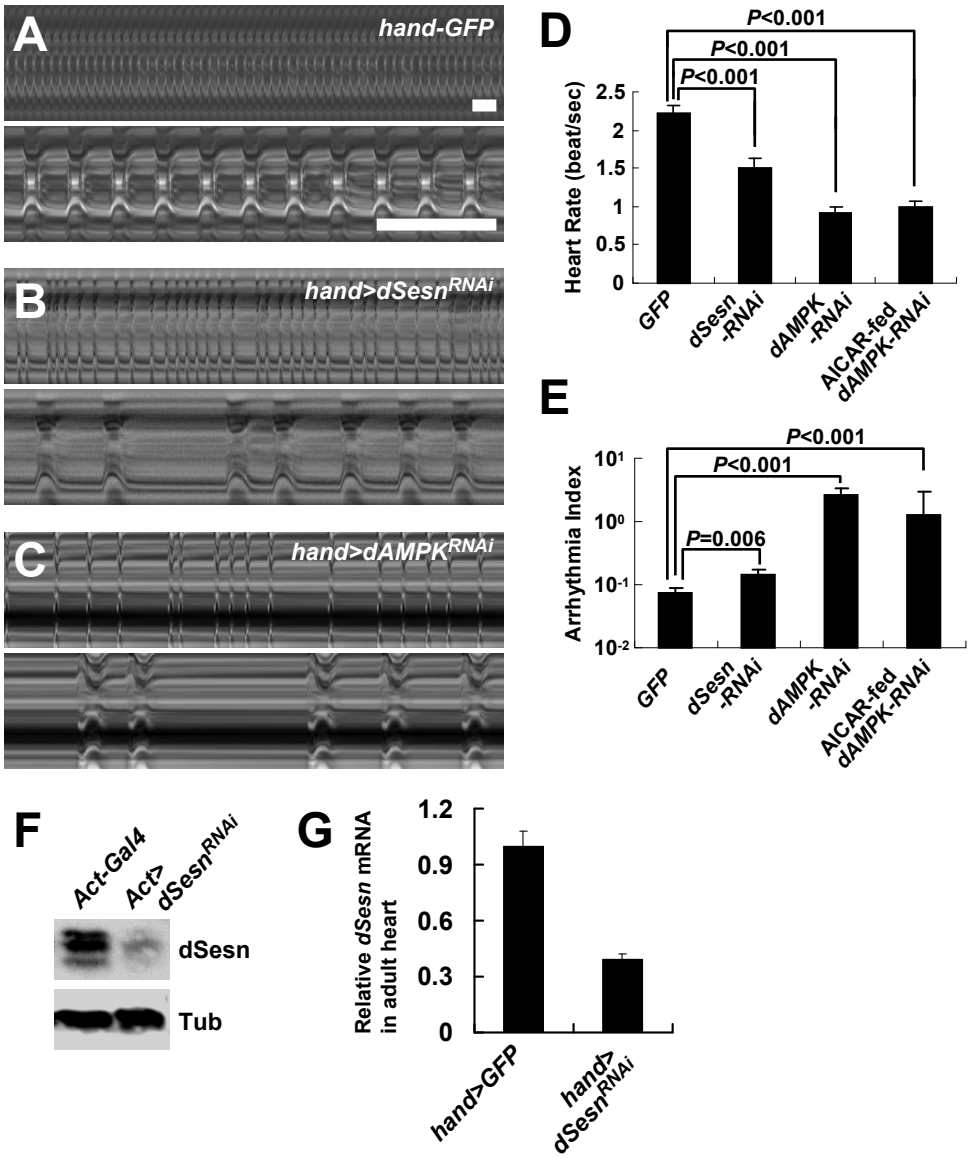
A
hand-GFP
B
hand>dSesn^RNAi
C
hand>dAMPK^RNAi
D
P<0.001
P<0.001
P<0.001
Heart Rate (beat/sec)
2.5
2
1.5
1
0.5
0
GFP
dSesn -RNAi
dAMPK -RNAi
AICAR-fed dAMPK-RNAi
E
P<0.001
P<0.001
P=0.006
Arrhythmia Index
10^1
10^0
10^-1
10^-2
GFP
dSesn -RNAi
dAMPK -RNAi
AICAR-fed dAMPK-RNAi
F
Act-Gal4
Act> dSesn^RNAi
dSesn
Tub
G
Relative dSesn mRNA in adult heart
1.2
0.9
0.6
0.3
0
hand>GFP
hand> dSesn^RNAi

Fig. S17

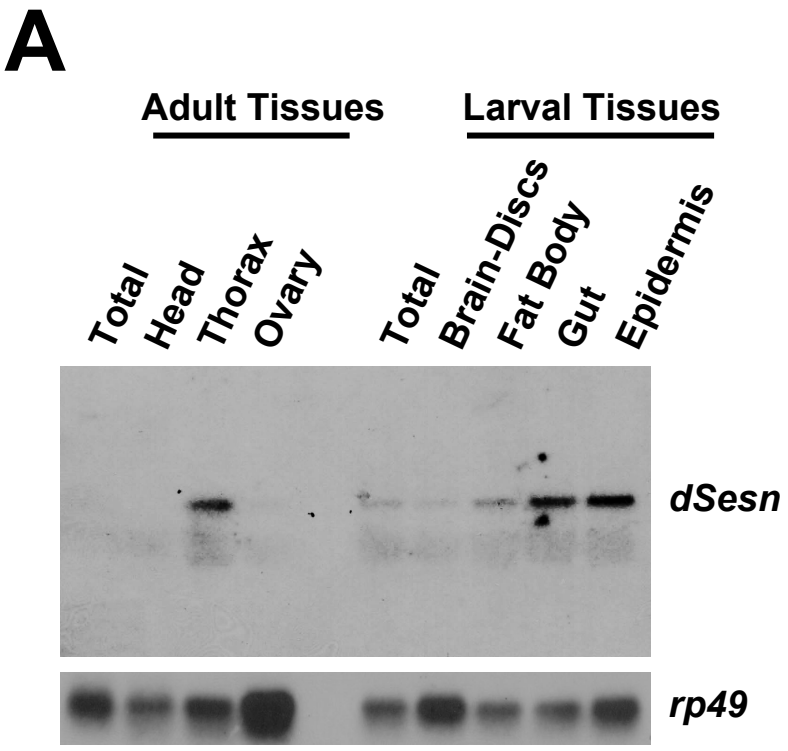
A
Adult Tissues
Larval Tissues
Total
Head
Thorax
Ovary
Total
Brain-Discs
Fat Body
Gut
Epidermis
dSesn
rp49

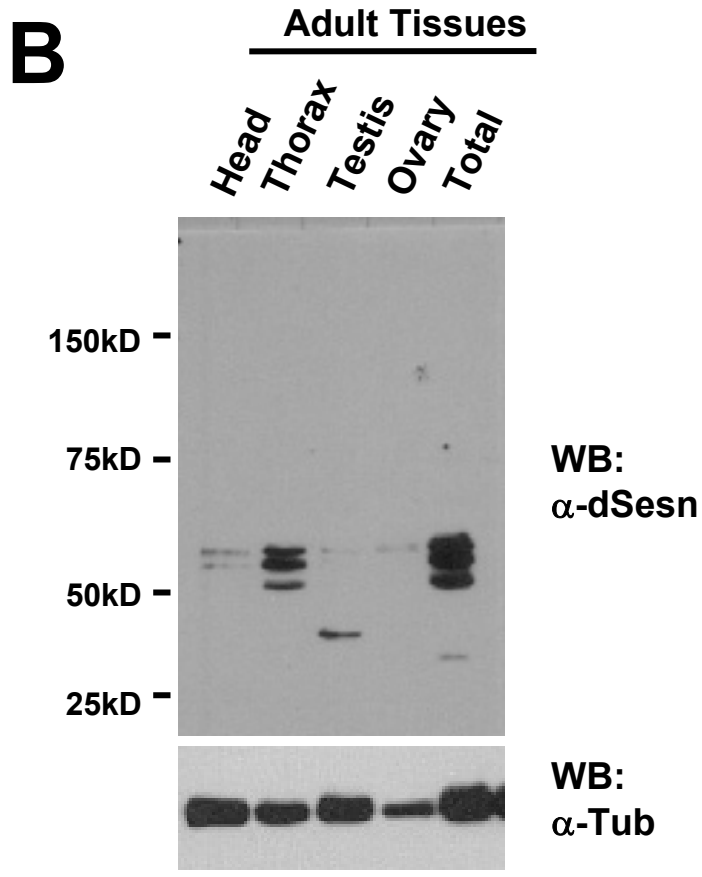
B
Adult Tissues
Head
Thorax
Testis
Ovary
Total
150kD
75kD
50kD
25kD
WB:
α-dSesn
WB:
α-Tub

Fig. S18

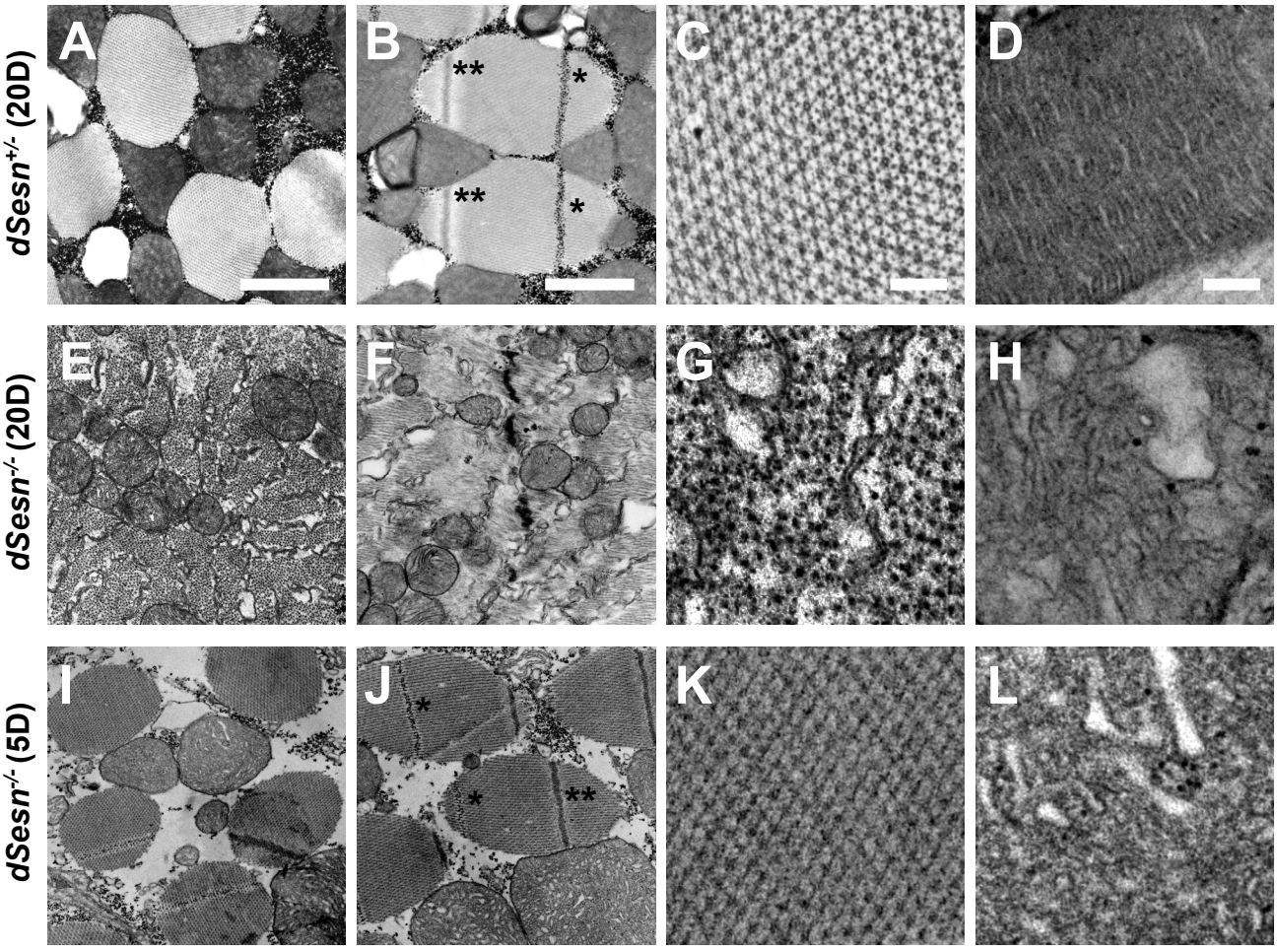

Fig. S19

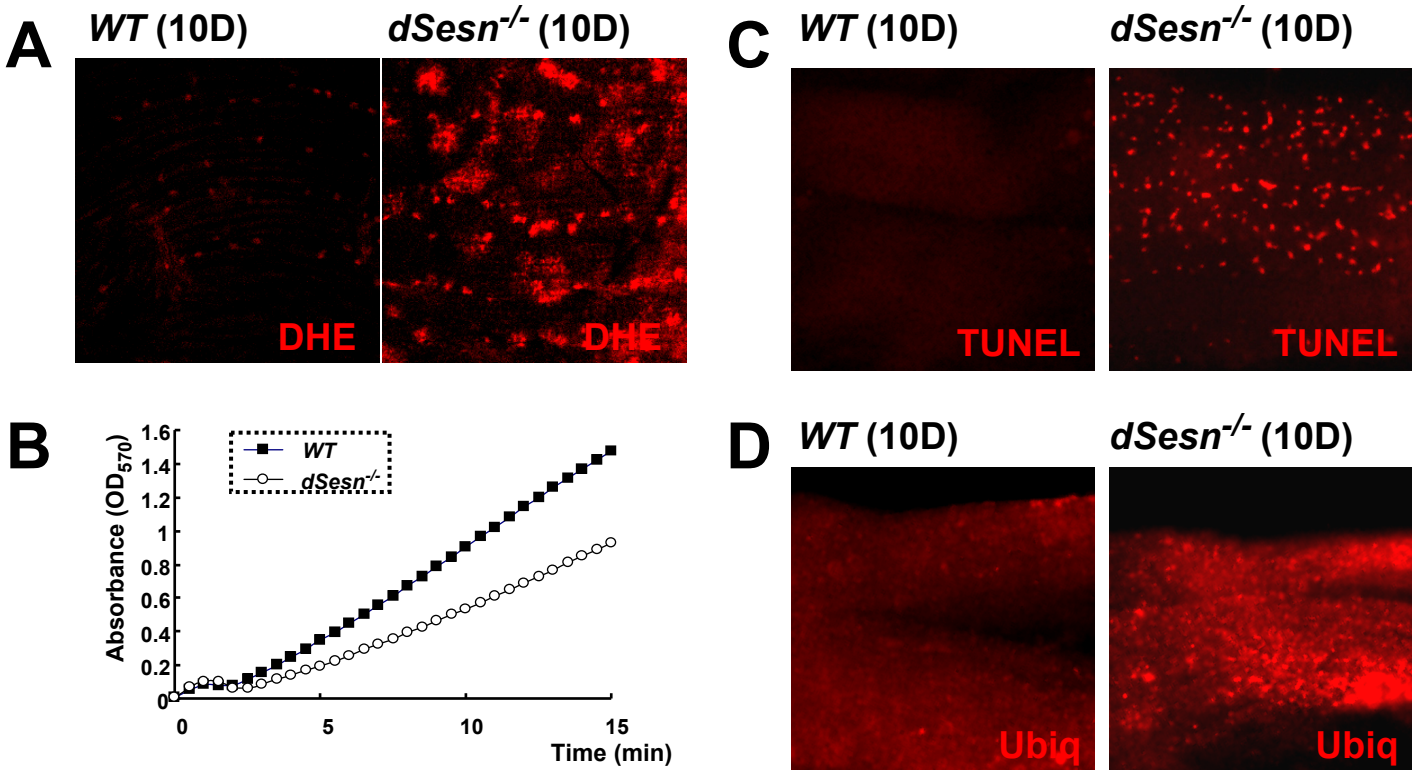
A
WT (10D)
dSesn-/- (10D)
DHE
DHE
B
WT
dSesn-/-
Absorbance (OD570)
0
0.2
0.4
0.6
0.8
1
1.2
1.4
1.6
0
5
10
15
Time (min)
C
WT (10D)
dSesn-/- (10D)
TUNEL
TUNEL
D
WT (10D)
dSesn-/- (10D)
Ubiq
Ubiq

Fig. S20

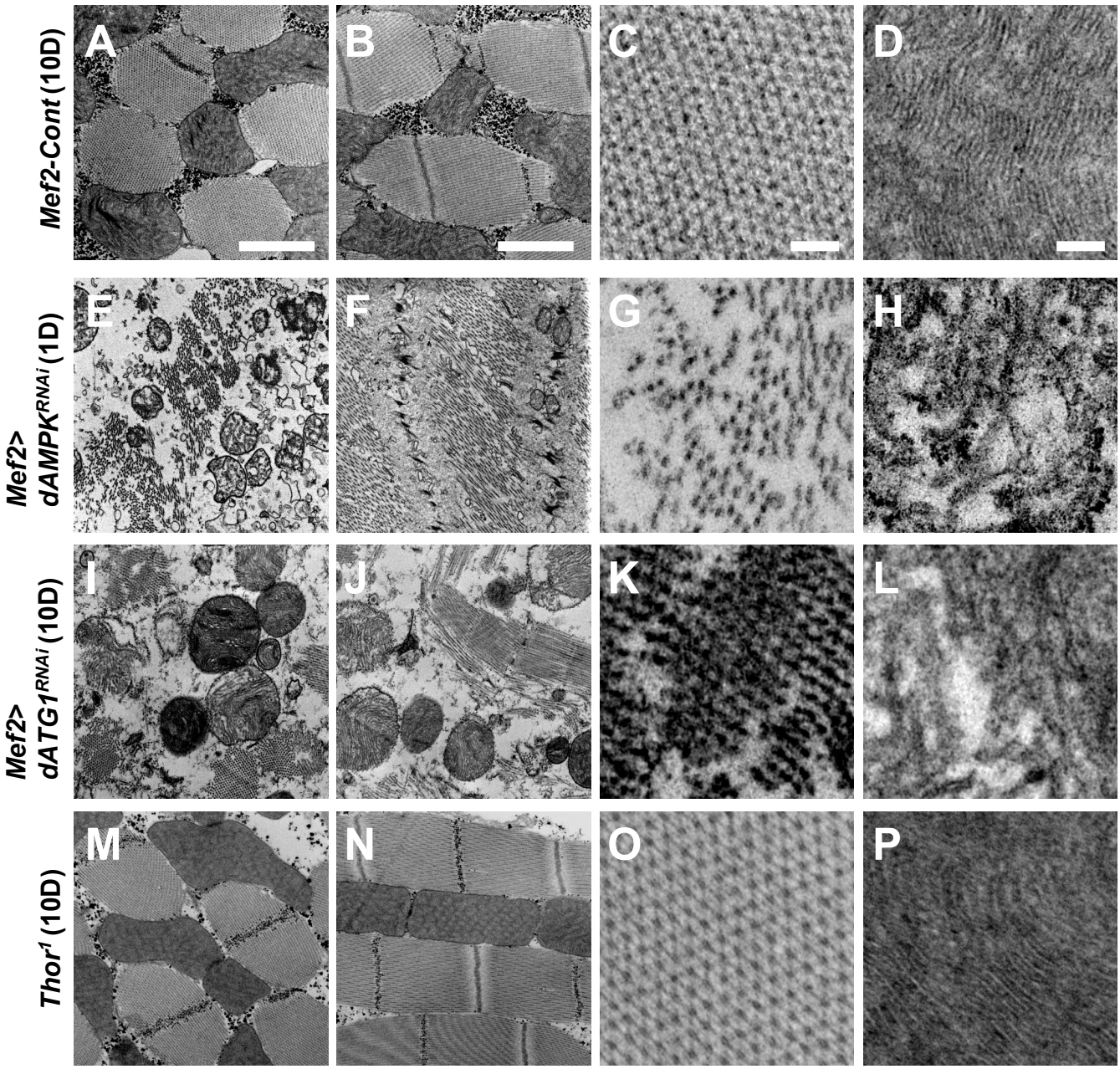
Mef2-Cont (10D)
Mef2> dAMPK^RNAi (1D)
Mef2> dATG1^RNAi (10D)
Thor^1 (10D)
A
B
C
D
E
F
G
H
I
J
K
L
M
N
O
P

Fig. S21